

Neutrino Degeneracy and Decoupling: New Limits from Primordial Nucleosynthesis and the Cosmic Microwave Background

M. Orito¹, T. Kajino^{1,2,3}, G. J. Mathews^{1,4}, and R. N. Boyd⁵

ABSTRACT

We reanalyze the cosmological constraints on the existence of a net universal lepton asymmetry and neutrino degeneracy. We show that neutrinos can begin to decouple at higher temperatures than previous estimates due to several corrections which diminish the neutrino reaction rate. For sufficiently large degeneracy, neutrino decoupling can occur before various particles annihilate and even before the QCD phase transition. These decoupled neutrinos are therefore not heated as the particle degrees of freedom change. The resultant ratio of the relic neutrino-to-photon temperatures after e^\pm annihilation can then be significantly reduced by more than a factor of two from that of the standard nondegenerate ratio. This changes the expansion rate and subsequent primordial nucleosynthesis, photon decoupling, and structure formation. In particular we analyze physically plausible lepton-asymmetric models with large ν_μ and ν_τ degeneracies together with a moderate ν_e degeneracy. We show that the nucleosynthesis by itself permits very large neutrino degeneracies $0 \leq \xi_{\nu_\mu}, \xi_{\nu_\tau} \leq 40$, $0 \leq \xi_{\nu_e} \leq 1.4$ together with large baryon densities $0.1 \leq \Omega_b h_{50}^2 \leq 1$ as long as some destruction of primordial lithium has occurred. We also show that structure formation and the power spectrum of the cosmic microwave background allows for the possibility of an $\Omega = 1$, $\Omega_\Lambda = 0.4$, cosmological model

¹ National Astronomical Observatory, 2-21-1, Osawa, Mitaka, Tokyo 181-8588, Japan

² Graduate University for Advanced Studies, Department of Astronomical Science, 2-21-1, Osawa, Mitaka, Tokyo 181-8588, Japan

³ University of Tokyo, Department of Astronomy, 7-3-1 Hongo, Bunkyo-ku, Tokyo 113-0033, Japan

⁴ Center for Astrophysics, and Department of Physics, University of Notre Dame, Notre Dame, IN 46556

⁵ Department of Physics, Department of Astronomy, Ohio State University, Columbus, OH 43210

for which there is both significant lepton asymmetry ($|\xi_{\nu_\mu}| = |\xi_{\nu_\tau}| \approx 11$) and a relatively large baryon density ($\Omega_b h_{50}^2 \approx 0.2$). Our best-fit neutrino-degenerate, high-baryon-content models are mainly distinguished by a suppression of the second peak in the microwave background power spectrum. This is consistent with the recent high resolution data from BOOMERANG and MAXIMA-1.

Subject headings: cosmology: lepton asymmetry, Ω_b - cosmic microwave background

1. INTRODUCTION

The universe appears to be charge neutral to very high precision (Lyttleton & Bondi 1959). Hence, any universal net lepton number beyond the net baryon number must reside entirely within the neutrino sector. Since the present relic neutrino number asymmetry is not directly observable there is no firm experimental basis for postulating that the lepton number for each species is zero. It is therefore possible for the individual lepton numbers L_l of the universe to be large compared to the baryon number of the universe, B , while the net total lepton number is small ($L \sim B$). Furthermore, it has been suggested that even if the baryon number asymmetry is small, the total lepton number could be large in the context of $SU(5)$ and $SO(10)$ Grand Unified Theories (GUT's) (Harvey & Kolb 1981; Fry & Hogan 1982; Dolgov & Kirilova 1991; Dolgov 1992). It has also been proposed recently (Casas, Cheng, & Gelmini 1999) that models based upon the Affleck-Dine scenario of baryogenesis (Affleck & Dine 1985) might generate naturally lepton number asymmetry which is seven to ten orders of magnitude larger than the baryon number asymmetry. Neutrinos with large lepton asymmetry and masses ~ 0.07 eV might even explain the existence of cosmic rays with energies in excess of the Greisen-Zatsepin-Kuzmin cutoff (Greisen 1966; Gelmini & Kusenko 1999). Degenerate, massive (2.4 eV) neutrinos may even be required (Larsen & Madsen 1995) to provide a good fit to the power spectrum of large scale structure in mixed dark matter models. It is, therefore, equally important for both particle physics and cosmology to carefully scrutinize the limits which cosmology places on the allowed range of both the lepton and baryon asymmetries.

The consequences of a large lepton asymmetry and associated neutrino degeneracy for big bang nucleosynthesis (BBN) have been considered in many papers. Models with degenerate ν_e (Wagoner, Fowler, & Hoyle 1967; Terasawa & Sato 1985; Scherrer 1983; 1988; Kajino & Orito 1998a), both ν_e and ν_μ (Yahil & Beaudet 1976; Beaudet & Goret 1976; Beaudet & Yahil 1977), and for three degenerate neutrino species (David & Reeves 1980;

Olive et al. 1991; Kang & Steigman 1992; Starkman 1992; Kajino & Orito 1998b; Kim & Lee 1995; Kim, Kim & Lee 1998) have been analyzed. The effects of the degeneracy of electron type neutrinos on inhomogeneous BBN models were also considered in Kajino & Orito (1998a, 1998b). Constraints on lepton asymmetry also arise from the requirement that sufficient structure develop by the present time (Kang & Steigman 1992) and from the power spectrum of fluctuations in galaxies (Larsen & Madsen 1995) and the cosmic microwave background temperature (Kinney & Riotto 1999; Lesgourgues & Pastor 1999; Hannestad 2000).

The present work differs from those listed above primarily in that we carefully reexamine the neutrino decoupling temperature. Although neutrino degeneracy has been treated in considerable detail previously (cf. Kang & Steigman 1992) we reexamine several issues which were not treated in that paper or elsewhere. We show that there are corrections to the neutrino reaction rates which cause the neutrino decoupling temperature to be significantly higher than previous estimates. These corrections include a proper accounting of effects of degeneracy on the abundances of the weakly-reacting species present. We also consider corrections in the the electron and photon effective masses and the relative velocities of interacting species. In addition we make a more careful continuous treatment of the various particle annihilation epochs. These corrections are important since it becomes easier for neutrinos to decouple before the annihilation of various particles and even before the QCD transition. The fact that neutrinos may decouple when there were many particle degrees of freedom causes the relic neutrino temperature to be much lower than that of the standard nondegenerate big bang. This allows for new solutions for BBN in which significant baryon density is possible without violating the various abundance constraints. We find that for decoupling temperatures just above the QCD epoch it is also possible to find models in which the structure constraint and even the CMB power spectrum constraint are marginally satisfied.

In this paper we explore a physically plausible range of baryon and lepton asymmetric cosmological models in which the electron neutrino is only slightly degenerate while the muon and tau neutrinos have nearly equal (but opposite-sign) significant chemical potentials. We use these models to deduce new cosmological constraints on the baryon and lepton content of the universe. We emphasize that previous studies of BBN and the CMB temperature fluctuations with highly degenerate neutrinos have not exhaustively scrutinized the possibility of important effects from the lower implied neutrino temperature when neutrinos decouple before various particle annihilations and/or the QCD epoch.

In what follows we first discuss here how the observable BBN yields in a neutrino-degenerate universe impose bounds on the baryon and lepton asymmetries which still

allow a large neutrino degeneracy and baryon density (even $\Omega_b = 1$). We show that there exists a one parameter family of allowed neutrino-degenerate models which satisfy all of the constraints from BBN. We next examine other cosmological non-nucleosynthesis constraints, i.e. the cosmic microwave background (CMB) fluctuations and the time scale for the development of structure. We show that these constraints can be marginally satisfied for a limited range of highly degenerate models from the fact the relic neutrino temperature is much lower than that of the standard nondegenerate big bang. We also discuss how a determination of the neutrino degeneracy parameters could constrain the neutrino mass spectrum from the implied neutrino contribution Ω_ν to the closure density.

2. LEPTON ASYMMETRY & NEUTRINO DECOUPLING

In this section, we review the basic relations which define the magnitude of neutrino degeneracy and summarize the cosmological implications. Radiation and relativistic particles dominate the evolution of the early hot big bang. In particular, relativistic neutrinos with masses less than the neutrino decoupling temperature, $m_\nu \lesssim \mathcal{O}(T_D) \sim \text{MeV}$, contributed an energy density greater than that due to photons and charged leptons. Therefore, a small modification of neutrino properties can significantly change the expansion rate of the universe. The energy density of massive degenerate neutrinos and antineutrinos for each species is described by the usual Fermi-Dirac distribution functions f_ν and $f_{\bar{\nu}}$,

$$\rho_\nu + \rho_{\bar{\nu}} = \frac{1}{2\pi^2} \int_0^\infty dp p^2 \sqrt{p^2 + m_\nu^2} (f_\nu(p) + f_{\bar{\nu}}(p)). \quad (1)$$

where, p denotes the magnitude of the 3-momentum, and m_ν is the neutrino mass. Here and throughout the paper we use natural units ($\hbar = c = k_B = 1$). The distribution functions are

$$f_\nu(p) = \frac{1}{\exp(p/T_\nu - \xi_\nu) + 1}, \quad (2)$$

$$f_{\bar{\nu}}(p) = \frac{1}{\exp(p/T_\nu + \xi_\nu) + 1},$$

where the degeneracy parameter ξ_ν is defined in term of the neutrino chemical potential, μ_ν , as $\xi_\nu \equiv \mu_\nu/T_\nu$. It will have a nonzero value if a lepton asymmetry exists. In the limit of massless neutrinos, the energy density in neutrinos becomes

$$\rho_\nu + \rho_{\bar{\nu}} = \frac{7\pi^2}{8 \cdot 15} \sum_i T_{\nu_i}^4 \left[1 + \frac{15}{7} \left(\frac{\xi_{\nu_i}}{\pi} \right)^4 + \frac{30}{7} \left(\frac{\xi_{\nu_i}}{\pi} \right)^2 \right], \quad (3)$$

from which it is clear that a neutrino degeneracy in any species tends to increase the energy density.

The net lepton asymmetry L of the universe can be expressed to high accuracy as

$$L = \sum_{l=e,\mu,\tau} L_l, \tag{4}$$

$$L_l = \frac{n_{\nu_l} - n_{\bar{\nu}_l}}{n_\gamma}.$$

This is analogous to the baryon-to-photon ratio $\eta \equiv (n_B - n_{\bar{B}})/n_\gamma$. Here, n_{ν_l} ($n_{\bar{\nu}_l}$) are the number densities for each neutrino (anti-neutrino) species, n_γ is the photon number density, and n_B ($n_{\bar{B}}$) is the (anti)baryon number density. Once the temperature drops sufficiently below the muon rest mass, say $T \lesssim 10$ MeV, all charged leptons except for electrons and positrons will have decayed away. Overall charge neutrality then demands that the difference between the number densities of electrons and positrons equal the proton number density. Hence, any electron degeneracy is negligibly small and any significant lepton asymmetry must reside in the neutrino sector. After the epoch of e^\pm annihilation, the magnitudes of the lepton and baryon asymmetries are conserved. They are equal to the present value in the absence of any subsequent baryon and/or lepton number-violating processes.

Elastic scattering reactions, such as $\nu_l (\bar{\nu}_l) + l^\pm \leftrightarrow \nu_l (\bar{\nu}_l) + l^\pm$, keep the neutrinos in kinetic equilibrium. Annihilation and creation processes which can change their number density, like $\nu_l + \bar{\nu}_l \leftrightarrow l + \bar{l}$, $\nu_l + l' \leftrightarrow \nu_{l'} + l$, etc, maintain the neutrinos in chemical equilibrium. When the rates for these weak interactions become slower than the Hubble expansion rate, neutrinos decouple and begin a "free expansion". Their number densities continue to diminish as $1/R^3$ and their momenta red-shift by a factor $1/R$, where R is the cosmic scale factor. However, this decoupling has no effect on the shape of the distribution functions. Relativistic neutrinos and antineutrinos continue to be described by the Fermi-Dirac distributions of Eq. (2). Since the individual lepton number is believed to be conserved, the degeneracy parameters ξ_{ν_l} remain constant after decoupling.

2.1. Neutrino Decoupling Temperature

When one estimates the present density of relic neutrinos one must consider the effect of the changing number of degrees of freedom for the remaining interacting particles. For example, once the neutrinos are totally decoupled, they are not heated by subsequent pair annihilations. Hence, their temperature T_ν is lower than the temperature T_γ of photons (and

any other electromagnetically interacting particles) by a factor $y_\nu = T_\nu/T_\gamma$. In the standard non-degenerate cosmology, with three flavors of massless, non-degenerate neutrinos which decouple just before the e^\pm pair annihilation epoch, the present ratio of the neutrino to photon temperatures is given by $y_\nu = (4/11)^{1/3}$.

Neutrinos and anti-neutrinos drop out of thermal equilibrium with the background thermal plasma when the weak reaction rate per particle, Γ , becomes slower than the expansion rate, H . Since the decoupling occurs quickly, it is a good approximation to estimate a characteristic decoupling temperature T_D , at which the slowest weak-equilibrating reaction per particle Γ becomes slower than the expansion rate.

The expansion rate is simply given by the Friedmann equation

$$H = \sqrt{(8/3)\pi G \sum_i \rho_i} \quad , \quad (5)$$

where the sum is over all species contributing mass energy (mostly relativistic particles). Obviously, the universal expansion in neutrino-degenerate models is more rapid because of the higher neutrino mass-energy density (e.g. Equation 3). This causes the decoupling to occur sooner and at a higher temperature than in the non-degenerate case.

Our estimates of the weak decoupling temperature as a function of neutrino degeneracy are shown in Figure 1 and compared with the previous estimates Kang & Steigman (1992). Our decoupling temperatures are significantly higher than those estimated in Kang & Steigman (1992) for reasons which we now explain.

Significant neutrino degeneracy will cause the weak reaction rate per particle, Γ , to be slower than the nondegenerate case because the neutrino final states are occupied (Kang & Steigman 1992; Freese, Kolb, & Turner 1983). More importantly, the existence of a lepton asymmetry represented by a finite positive neutrino chemical potential will cause the number density of antineutrinos to be significantly less than that of neutrinos. Hence, the annihilation rate per neutrino $\Gamma_\nu = n_{\bar{\nu}} \langle \sigma_{\nu\bar{\nu}} \rangle$ can be significantly less than the reaction rate per antineutrino, electron or positron.

In Kang & Steigman (1992) the weak reaction rate was estimated from the reaction rate per electron annihilation, $e^+ + e^- \rightarrow \nu_i + \bar{\nu}_i$. We will call this Γ_e . One could however also consider the reaction rate per positron, Γ_{e^+} , the reaction rate per neutrino species i , Γ_{ν_i} , or the reaction rate per antineutrino, $\Gamma_{\bar{\nu}_i}$. In the limit of high temperature and no neutrino degeneracy, all of these reaction rates are identical. However, when for example the neutrinos have a large positive chemical potential, the neutrino annihilation rate $\Gamma_{\nu_i} = n_{\bar{\nu}_i} \langle \sigma_{\nu\bar{\nu}} \rangle$ becomes the rate determining reaction. This is because of the scarcity of anti-neutrinos with which to interact. It is then this reaction rate and not Γ_e which should

be used to determine when the weak reactions are no longer able to maintain chemical equilibrium.

In Kang & Steigman (1992) expressions were derived for the phase space integrals for $\langle\sigma v\rangle$ which reduce to

$$\langle\sigma v\rangle = \frac{8(a^2 + b^2)}{27\pi\zeta^2(3)} I(\xi) G_F T^2 \quad , \quad (6)$$

where $I(\xi)$ is a phase space integration factor given in that paper, ζ is the Riemann zeta function, and G_F is the Fermi coupling constant. The quantities a and b relate to the Weinberg angle, $a = 1/2 + 2\sin^2\theta_W$ for electron neutrinos, and $a = 1/2 - 2\sin^2\theta_W$ for muon and tau neutrinos, while $b = 1/2$.

Using this, we derive the following expression for the decoupling temperature corresponding to each neutrino species, i ,

$$T_D(\xi_i) \approx \left[\frac{4.38}{a^2 + b^2} \right]^{1/3} \left[\frac{\sqrt{g'_{eff}(\xi)}}{I(\xi)} \right]^{1/3} \times \left(\frac{n_{\bar{i}}}{n_e} \right)^{1/3} \text{ MeV} \quad , \quad (7)$$

where \bar{i} denotes the matter (or antimatter) counter part for the species under consideration. The formula A.8 of Kang & Steigman (1992) omits the latter density ratio factor which is only unity in the limit of no degeneracy. Thus, their Γ used to deduce the decoupling temperature was too large. We have checked the above result against a full eight-dimensional integration of the Boltzmann equation and find our results to be correct.

There are also two other differences between our results and those of Kang & Steigman (1992): The first is that we have included finite temperature corrections to the mass of the electron and photon (Fornengo, Kim, & Song 1997). The second is that we have calculated the average neutrino annihilation rate in the cosmic comoving frame. In this frame the Møller velocity is used instead of the relative velocity for the integration of the collision term in the Boltzmann equations (Gondolo, & Gelmini 1991; Enqvist et al. 1992). These corrections also slightly increase the neutrino decoupling temperatures. Therefore even in the nondegenerate case we find slightly higher decoupling temperatures than those of Kang & Steigman (1992):

$$\begin{aligned} T_D(\xi_\nu = 0) &\simeq 2.33 \text{ MeV} \quad \text{for } \nu_e \quad , \\ T_D(\xi_\nu = 0) &\simeq 3.90 \text{ MeV} \quad \text{for } \nu_{\mu,\tau} \quad . \end{aligned} \quad (8)$$

These values are in good agreement with those of Enqvist et al. (1992). If we remove the above corrections, we recover the decoupling temperatures of (Kang & Steigman 1992), i.e. $T_D(\xi_\nu = 0) \simeq 1.98 \text{ MeV}$ for ν_e , and $T_D(\xi_\nu = 0) \simeq 3.30 \text{ MeV}$ for $\nu_{\mu,\tau}$.

2.2. Relic Neutrino Temperature

One does not need to increase the decoupling temperature by much before photon heating by annihilations becomes important for determining the relic neutrino temperature. For illustration, Figure 2 shows the ratio of muon to photon energy densities as a function of temperature in units of the muon rest mass $m_\mu = 105$ MeV. A similar curve could be drawn for any massive species. One can see that even at a temperature of only 20% of the muon rest mass, muons still contribute about 10% of the mass energy density, and hence, can affect the ratio of the photon to neutrino temperatures as these remaining muons annihilate. Combining Figures 1 and 2, one can see that even for a degeneracy parameter of $\xi_\nu \sim 6$, the decoupling temperature is at 20% of m_μ . For the case of highly degenerate neutrinos ($\xi_{\nu_\mu} \gtrsim 10.8$ and $\xi_{\nu_\tau} \gtrsim 9.8$), $T_D(\xi_{\nu_i})$ can exceed the muon rest energy and even the QCD phase transition temperature.

If the neutrinos decouple early, they are not heated as the number of particle degrees of freedom change. Hence, the ratio of the neutrino to photon temperatures, T_ν/T_γ , is reduced. The computation of the ratio of the final present neutrino temperature to the photon temperature is straightforward. Basically, since the universe is a closed system, the relativistic entropy is conserved within a comoving volume. That is;

$$R^3 s = \text{Constant} \quad , \quad (9)$$

where the entropy density s is defined,

$$s \equiv \sum \frac{(\rho_i + p_i - \mu_i n_i)}{T} = \frac{2\pi^2}{45} g_{eff} T^3 \quad , \quad (10)$$

and the sum is over all species present. Since the mass-energy is dominated by relativistic particles s can be written in terms of the effective number of particle degrees of freedom,

$$g_{eff} = \sum_{i=bosons} g_i \left(\frac{T_i}{T}\right)^3 + \frac{7}{8} \sum_{i=fermions} g_i \left(\frac{T_i}{T}\right)^3 \quad . \quad (11)$$

As each species annihilates, sR^3 remains constant. Therefore, the temperature of the remaining species increases by a factor of $(g_{eff}^{before}/g_{eff}^{after})^{1/3}$. This accounts for the usual heating of photons relative to neutrinos due to e^\pm pair annihilations by a factor of $(11/4)^{1/3}$. Note, that in the computation of g_{eff} from equations (10) and (11) it is important to evaluate the energy densities continuously (cf. Figure 2) and not simply assume abrupt annihilation as the temperature approaches the rest energy of each particle as was done in Kang & Steigman (1992).

Figure 3 illustrates g_{eff} as a function of temperature from 1 MeV to 1 TeV. In each calculation g_{eff} depends upon the relic neutrino temperature and therefore when the

neutrinos decoupled. For purposes of illustration only, we drawn this figure for three neutrino types which do not decouple until \approx MeV. To construct this figure we have included: mesons ($\pi, \rho, \phi, \omega, \eta, \eta'$); leptons ($e, \mu, \tau, \nu_e, \nu_\mu, \nu_\tau$); a QCD phase transition at 150 MeV; light quarks and gluons ($u, d, gluon$); s-quarks (with $m_s = 120$ MeV); c-quarks (with $m_c = 1200$ MeV); b-quarks (with $m_b = 4250$ MeV); W, Z-bosons (with $m_Z = 80$ GeV); and t-quarks (with $m_t = 173$ GeV).

One can see from this figure that if neutrinos decouple before the QCD phase transition, there is substantial heating of photons due to the large change in degrees of freedom at this epoch.

Figure 4 shows the final ratio of neutrino temperature today to that of the standard non-degenerate big bang for three neutrino flavors. The biggest drop in temperature for all three neutrino flavors occurs for $\xi_\nu \approx 10$. This corresponds to a decoupling temperature above the cosmic QCD phase transition. The low temperature is the result of the decrease in particle degrees of freedom during this phase transition. This discontinuity will have important consequences in the subsequent discussions.

For comparison, the same computation from Figure 1 of Kang & Steigman (1992) is shown. One can see that there is a substantial difference between the two results. These differences stem from two effects. On the one hand the decoupling temperature is higher in the present work for a given ξ_{ν_i} because of the various corrections as explained above. This is the reason that the discontinuity in relic neutrino temperature occurs at $\xi_{\nu_{\mu,\tau}} \approx 11$ instead of 15 as in Kang & Steigman (1992). The second difference is that here we have calculated the proper thermodynamic energy density for each fermion and boson species continuously (cf. Eq. 1), whereas in Kang & Steigman (1992) an approximation was made that each particle species instantaneously annihilates as the temperature drops below its rest energy. This is the reason for the step function appearance of the curve in Kang & Steigman (1992).

Some discussion of book keeping here is in order as it explains why we observe the jump in relic temperature when neutrinos decouple above the QCD transition. Let us consider a neutrino which decouples just above the QCD transition. Then the relevant fermion degrees of freedom consist mainly of 3 $q - \bar{q}$ colors (treating the s -quark as relativistic) \times 3 flavors contributing $g_f = 31.5$, plus $e^+ - e^-$ and $\mu^+ - \mu^-$ plus 2 remaining nondecoupled flavors of $\nu - \bar{\nu}$ lepton pairs. These contributing another $g_f = 10.5$. For the bosons there are 8 gluons and 1 photon contributing a total $g_b = 18$. While the species are in equilibrium the total $g_{eff} = 60$. If no more species decouple before the electron pair annihilation epoch, the fermion degrees of freedom before electron-positron annihilation (at $T \approx 1$ MeV) include only 2 flavors of $\nu - \bar{\nu}$ plus $e^+ - e^-$ so that $g_f = 7$, while for bosons only

photons remain so that $g_b = 2$ and $g_{eff} = 9$. The relic neutrino temperature is therefore reduced by an additional factor due to these differences in particle degrees of freedom $(T_\nu/T_\gamma)/[4/11]^{1/3} = (9/60)^{1/3} \approx 0.53$ (cf. Figure 4).

For all three neutrino flavors the temperature begins to decrease relative to the standard value for a degeneracy parameter as small as $\xi \sim 5$. This is because some relic $\mu - \bar{\mu}$ pairs are still present even at temperatures well below the muon rest energy (cf. Figure 2). The first neutrino species to be affected as the degeneracy increases are the ν_μ and ν_τ . They decouple at a higher temperature than ν_e even in the standard nondegenerate big bang because the electrons continue to experience charged-current interactions to lower temperature. The muon neutrinos exhibit a slightly different behavior than ν_τ for degeneracy parameters $\xi_{\nu_\mu} > 5$ because the $\mu - \bar{\mu}$ density is large enough at the decoupling temperature for charged-current interactions to be significant. This maintains equilibrium for ν_μ to somewhat lower temperatures even for degenerate neutrinos. This causes the ν_μ decoupling temperature to be lower (cf. Figure 1) and the relic temperature to be slightly higher than the ν_τ temperature for degeneracy parameters between 5 and 9.

3. PRIMORDIAL NUCLEOSYNTHESIS

3.1. Current Status

Although the homogeneous BBN model has provided strong support for the standard hot big-bang cosmology, possible conflicts have emerged between the predictions of BBN abundances as the astronomical data have become more precise in recent years. One difficulty has been imposed by recent detections of a low deuterium abundance (Burles & Tytler 1998a; Burles & Tytler 1998b, see also Levshakov, Tytler, & Burles 1999) in Lyman- α absorption systems along the line of sight to high red-shift quasars. The low D/H favors a high baryon content universe and a high primordial ^4He abundance, $Y_p \gtrsim 0.244$. This is inconsistent with at least some of the reported constraints from measurements of a low primordial abundance of ^4He , $Y_p \approx 0.235 \pm 0.003$, in low-metallicity extragalactic H II regions (Olive & Steigman 1995; Steigman 1996; Hata et al. 1996; Olive, Steigman, & Skillman 1997; Kajino & Orito 1998a; Piembert & Piembert 2000). This situation is exacerbated by recent detailed analyses (Esposito et al. 1999; Lopez & Turner 1999) of the theoretical uncertainties in the weak interactions affecting the neutron to proton ratio at the onset of primordial nucleosynthesis. These results require a positive net correction to the theoretically determined ^4He mass fraction Y_p of +0.004 to +0.005 or $\sim 2\%$. We also note that the low deuterium abundance is marginally inconsistent with the ^7Li abundance inferred by measurements of lithium in Population II halo stars (Ryan et al. 1999; Kajino

et al. 2000). Significant depletion of lithium from these stars, or a lower reaction rate for primordial lithium production may be required.

Another potential difficulty has been imposed by recent X-ray observations of rich clusters (White et al. 1993; White & Fabian 1995; David, Jones, & Forman 1995; Bahcall, Lubin, & Dorman 1995). The implied baryonic contribution to the closure density is $0.08 \leq \Omega_b h_{50}^{3/2} / \Omega_M \leq 0.22$ (Tytler et al. 2000), where Ω_M is the total matter (dark plus visible) contribution, and h_{50} is the Hubble constant H_0 in units of $50 \text{ km s}^{-1} \text{ Mpc}^{-1}$. Consistency with the limits ($0.03 \leq \Omega_b h_{50}^2 \leq 0.06$) from homogeneous BBN (Walker et al. 1991; Smith et al. 1993; Copi, Schramm & Turner 1995; Schramm & Mathews 1995; Olive, Steigman, & Walker 1999) then requires that $0.14 \leq \Omega_M h_{50}^{1/2} \leq 0.75$. Hence, matter dominated cosmological models (for example with $H_0 = 75 \text{ km s}^{-1} \text{ Mpc}^{-1}$ and $\Omega_M \geq 0.61$) can be in conflict with BBN.

Another possible conflict has emerged in recent measurements of the power spectrum of the cosmic microwave background (CMB) temperature fluctuations. A suppression of the second acoustic peak in the power spectrum has been recently reported in the balloon based CMB sky maps from the BOOMERANG (Bernardls, P. et al. 2000) and MAXIMA-1 (Hanany et al. 2000) collaborations. Indeed, the derivation of cosmological parameters from these new data sets (Lange et al. 2000; Balbi et al. 2000) indicate a preference for a large baryon density. For example, the optimum cosmological models consistent with the BOOMERANG data (Lange et al. 2000) indicate $\Omega_b h^2 = 0.032 \pm 0.004$ (1σ) for fits in which there is no prior restriction on the range of $\Omega_b h^2$. Similarly, the likelihood analysis based upon the MAXIMA-1 data (Balbi et al. 2000) indicates $\Omega_b h^2 = 0.025 \pm 0.005$. These results are to be compared with the best current (1σ) limit from standard primordial nucleosynthesis without neutrino degeneracy, $\Omega_b h^2 = 0.019 \pm 0.0024$ (Olive, Steigman, & Walker 1999; Tytler et al. 2000) which come from the deuterium abundance in Lyman- α clouds observed along the line of sight to background quasars. The CMB data indicate a baryon content which is at least $1\text{-}2 \sigma$ above the optimum BBN value. Indeed, $\Omega_b h^2 \geq 0.20$ would require a primordial helium abundance of $Y_p \geq 0.25$ which is beyond even the most generous adopted limits from observation (Olive, Steigman, & Walker 1999). Thus, it seems that that the CMB data hint at (though not necessarily prove) the need for a modification of BBN which allows higher values of $\Omega_b h^2$ while still satisfying the constraints from light element abundances. Such conditions are easily satisfied by neutrino-degenerate models.

3.2. Neutrino-Degenerate BBN

Most previous works have only considered the effects of neutrino degeneracy on the light elements ^4He , D, and ^7Li . Recently, the predicted abundance of other elements such as ^6Li , ^9Be , and ^{11}B in a neutrino-degenerate universe were also studied (Kim & Lee 1995; Kim, Kim & Lee 1998). Here we investigate the effects of lepton asymmetry on the predicted abundances of heavier elements ($12 \leq A \leq 18$) as well as these light elements.

Non-zero lepton numbers primarily affect nucleosynthesis in two ways (Wagoner, Fowler, & Hoyle 1967; Terasawa & Sato 1985; 1988; Scherrer 1983; Yahil & Beaudet 1976; Beaudet & Goret 1976; Beaudet & Yahil 1977; David & Reeves 1980; Olive et al. 1991; Kang & Steigman 1992; Starkman 1992; Kajino & Orito 1998a; Kim & Lee 1995; Kim, Kim & Lee 1998). First, degeneracy in any neutrino species leads to an increased universal expansion rate independently of the sign of ξ_{ν_e} (cf. Eqs. 3 and 5). As a result, the weak interactions that maintain neutrons and protons in statistical equilibrium decouple earlier. This effect alone would lead to an enhanced neutron-to-proton ratio at the onset of the nucleosynthesis epoch and increased ^4He production.

Secondly, a non-zero electron neutrino degeneracy can directly affect the equilibrium n/p ratio at weak-reaction freeze out. The equilibrium n/p ratio is related to the electron neutrino degeneracy by $n/p = \exp\{-(\Delta M/T_{n \leftrightarrow p}) - \xi_{\nu_e}\}$, where ΔM is the neutron-proton mass difference and $T_{n \leftrightarrow p}$ is the freeze-out temperature for the weak reactions converting protons to neutrons and vice versa. This effect leads to either increased or decreased ^4He production, depending upon the sign of L_e or ξ_{ν_e} .

There is also a third effect which we emphasize in this paper. As discussed in the previous section, T_ν/T_γ can be reduced if the neutrinos decouple at an earlier epoch. This lower temperature reduces the energy density of the highly degenerate neutrinos during the BBN era, and hence, slows down the expansion of the universe. This leads to decreased ^4He production. We show in the next section that the allowed values for $\xi_{\nu_e}, \xi_{\nu_\mu}, \xi_{\nu_\tau}$ and Ω_b which satisfy the light-element abundance constraints are significantly changed for large degeneracy ($\xi_{\nu_\mu}, \xi_{\nu_\tau} \gtrsim 10$) compared to the results of previous studies.

3.3. Summary of Light-Element Constraints

The primordial light element abundances deduced from observations have been reviewed in a number of recent papers (Olive, Steigman, & Walker 1999; Nolett & Burles 2000; Steigman 2000; Tytler et al. 2000). There are several outstanding uncertainties. For primordial helium there is an uncertainty due to the fact that deduced abundances tend to

fall in one of two possible values, one high and the other low. Hence, for ${}^4\text{He}$ we adopt a wide range:

$$0.226 \leq Y_p \leq 0.247.$$

For deuterium there is a similar possibility for either a high or low value. Here, however, we adopt the generally accepted low values of Tytler et al. (2000),

$$2.9 \times 10^{-5} \leq \text{D}/\text{H} \leq 4.0 \times 10^{-5}.$$

For primordial lithium there is some uncertainty from the possibility that old halo stars may have gradually depleted their primordial lithium. Because of this possibility we adopt the somewhat conservative constraint:

$$1.26 \times 10^{-10} \leq {}^7\text{Li}/\text{H} \leq 3.5 \times 10^{-10}$$

3.4. Nucleosynthesis Model

As we shall see, shifts in the relic neutrino temperature can dramatically affect the abundance yields (Kajino & Orito 1998b). We now explore the parameter space of neutrino degeneracy and baryonic content to reinvestigate the range of models compatible with the constraints from light element abundances.

For the present work we have applied a standard big bang code with all reactions updated up to $A=18$. [However, in the present discussion only reactions involving nuclei up to $A=15$ are significant.] In this way possible effects of lepton asymmetry on heavier element abundances could be analyzed along with the light elements. In this context a recent compilation of the nuclear reaction rates relevant to the production of ${}^{11}\text{B}$ (Orito, Kajino, & Oberhummer 1998) was useful because several important $\text{LiBeB}(a,x)$ and (n,γ) reaction rates in the literature sometimes differ from one another by 2-3 orders of magnitude. The calculated abundances of heavier elements based upon these rates can also differ from one another by 1-2 orders of magnitude. We carry out BBN calculations which include all of the recent compilations of reaction rates relevant to the production of isotopes including those that are heavier than ${}^7\text{Li}$ up to ${}^{18}\text{O}$ (i.e. Orito, Kajino, & Oberhummer 1998; Mohr, Herndl, & Oberhummer 1999; Angulo et al. 1999; Herndl et al. 1999; Wagemans et al. 1999; and any other previous estimates are considered).

3.5. Neutrino Degeneracy Parameters

We have explored a broad range of the parameter space of neutrino-degenerate models. The main effects of the inclusion of either ν_μ or ν_τ degeneracy on BBN is an enhancement of energy density of the universe. The values for ξ_{ν_μ} and ξ_{ν_τ} primarily affect the expansion rate. This means that ξ_{ν_μ} and ξ_{ν_τ} are roughly interchangeable as far as their effects on nucleosynthesis are concerned. Furthermore, we expect that the net total lepton number is small though the lepton number for individual species could be large. Hence, it is perhaps most plausible to assume that the absolute values of $|\xi_{\nu_\mu}|$ and $|\xi_{\nu_\tau}|$ are nearly equal. Therefore, in what follows, we describe results for $|\xi_{\nu_\mu}| = |\xi_{\nu_\tau}| \equiv \xi_{\nu_{\mu,\tau}}$. This reduces the parameter space to three quantities: Ω_b , ξ_{ν_e} , and $|\xi_{\nu_\mu}| = |\xi_{\nu_\tau}|$. The calculations were conducted by first choosing a value for $\Omega_b h_{50}^2$. It was then necessary to find a value of ξ_{ν_e} for which the light element constraints could be satisfied for some value of $\xi_{\nu_{\mu,\tau}}$.

3.6. Results

As an illustration, Figure 5 shows a calculations of the helium abundance as a function of $\xi_{\nu_{\mu,\tau}}$ in a model with $\Omega_b h_{50}^2 = 0.3$. It was found in this model that the helium constraint could be satisfied for ξ_{ν_e} in the range of 0.79 to 0.94. This figure is for $\xi_{\nu_e} = 0.9$. Our results for $\xi_{\nu_{\mu,\tau}} < 10$ are consistent with those of Kang & Steigman (1992) if we run for a similar baryon-to-photon ratio $\eta_{10} = 5$ or 100 and utilize the neutron half life adopted in that paper.

In our calculations for helium (Figure 5) and other light nuclides (Figure 6) we see two different jumps in the nucleosynthesis yields. There is a small one for $\xi_{\nu_{\mu,\tau}} \approx 10$ and a large one for $\xi_{\nu_{\mu,\tau}} \approx 11.4$. These two jumps are due to the fact that we consider two degenerate neutrino species which decouple at slightly different temperatures (due to the presence of muons to interact with ν_μ). Therefore, one species (ν_τ) decouples above the QCD transition for a smaller value for $\xi_{\nu_{\mu,\tau}}$. However, this jump has a smaller effect on nucleosynthesis because so many degrees of freedom are still carried by the other degenerate neutrino species (ν_μ) which decouples later.

The main difference between our results and Kang & Steigman (1992), however, is that the helium abundance is significantly changed at high values of $\xi_{\nu_{\mu,\tau}}$. This results from our higher decoupling temperatures and therefore the lower relic neutrino temperatures during primordial nucleosynthesis (See Figure 4). This effect of varying T_ν/T_γ for large ξ_ν on BBN has not been adequately explored in the previous studies.

Figure 6 illustrates the effects on the other light-element abundances for this particular

parameter set. This figure shows that for moderate values of $\xi_{\nu_{\mu,\tau}}$ the main effect is that weak reaction freeze-out occurs at a higher temperature. The resultant enhanced n/p ratio increases the abundances of the neutron-rich light elements, D, ^3H and ^7Li , while the ^7Be abundance decreases.

Regarding ^7Li and ^7Be , the enhanced expansion rate from neutrino degeneracy affects the yield of $A = 7$ elements in two different ways. These elements are produced mainly by the nuclear electromagnetic capture reactions: $t(\alpha, \gamma)^7\text{Li}$ and $^3\text{He}(\alpha, \gamma)^7\text{Be}$. Hence, the production of these elements begins at a later time and lower temperature than the other light elements because they require time for a significant build up of the reacting $A = 3$ and 4 elements. In a neutrino-degenerate universe, however, the increased expansion rate, hastens the freeze-out of these reactions from nuclear statistical equilibrium (NSE) resulting in reduced $A = 7$ yields relative to the nondegenerate case. However, the enhanced n/p ratio also increases the tritium abundance in NSE. This effect tends to offset the effect of rapid expansion on the production of ^7Li . The net result is more ^7Li production.

As in the case of primordial helium, there is a rapid change in the nucleosynthesis yields on Figure 6 once the ν_{μ} and ν_{τ} decoupling temperatures separately exceed the epoch of the QCD phase transition. The ensuing lower neutrino temperature during primordial nucleosynthesis then resets the abundances to those of a lower effective degeneracy. The two discontinuities in Figure 6 at $\xi_{\nu_{\mu,\tau}} = 10$ and 11.4 correspond to the points at which respectively the tau or muon neutrino decoupling temperatures separately exceed the QCD phase transition temperature (cf. Figure 4).

Figure 7(a) summarizes the allowed regions of the ξ_{ν_e} vs. $\xi_{\nu_{\mu,\tau}}$ plane based upon the various indicated light element constraints in a universe with $\Omega_b h_{50}^2 = 0.1$. The usually identified allowed region (cf. Kohri, Kawasaki, & Sato 1997) for small $\xi_{\nu_e} \sim 0.2$ and $\xi_{\nu_{\mu,\tau}} \sim 2$ is apparent. Indeed, it has been argued (cf. Kohri, Kawasaki, & Sato 1997) that such degeneracy may be essential to explain the differences in the constraints from primordial helium and deuterium.

Figures 7(b) and 7(c) show the same plots, but for $\Omega_b h_{50}^2 = 0.2$ and $\Omega_b h_{50}^2 = 0.3$, respectively. The decline in the primordial deuterium abundance for models in which $\xi_{\nu_{\mu,\tau}} > 10$ allows for new regions of the parameter space in which the light element constraints can be accommodated. This new allowed region for large degeneracy persists as the baryon density is increased.

Figure 8 highlights the basic result of this study. It shows that there exists a single parameter (either $\xi_{\nu_{\mu,\tau}}$ or $\Omega_b h_{50}^2$) family of neutrino degenerate models allowed by BBN. For low $\Omega_b h_{50}^2$ models, only the usual low values for ξ_{ν_e} and $\xi_{\nu_{\mu,\tau}}$ are allowed. Between $\Omega_b h_{50}^2 \approx$

0.187 and 0.3, however, more than one allowed region emerges. For $\Omega_b h_{50}^2 \gtrsim 0.4$ only the large degeneracy solution is allowed. Neutrino degeneracy can even allow baryonic densities up to $\Omega_b h_{50}^2 = 1$. This result has been noted previously (cf. Kang & Steigman 1992; Starkman 1992). What is different here is that the high $\Omega_b h_{50}^2$ models are made possible for smaller values of ξ_{ν_e} due to the higher neutrino decoupling temperatures deduced in the present work. As we shall see, this allows the circumvention of other cosmological constraints as well suggesting that baryons and degenerate neutrinos might provide a larger contribution to the universal closure density than has previously been derived.

Figures 9-11 illustrate the elemental abundances obtained in the family of allowed models as a function of $\Omega_b h_{50}^2$. Figure 11 in particular allows us to consider whether there exists an abundance signature in other elements which might distinguish this new degenerate neutrino solution from standard BBN. For the most part the yields of the light and heavy species are similar to those of the standard non-degenerate big bang. However, the boron abundance exhibits an increase with baryon density due to alpha captures on ${}^7\text{Li}$. Thus, in principle, an anomalously high boron abundance together with beryllium and ${}^6\text{Li}$ similar to that expected from standard BBN might be a signature of neutrino-degeneracy.

4. OTHER COSMOLOGICAL CONSTRAINTS

We have seen that a new parameter space in the constraints from light elements on BBN emerges in neutrino-degenerate models just from the fact that the relic neutrino temperature is substantially diminished when degeneracy pushes neutrino decoupling to an earlier epoch. The viability of this solution requires large neutrino degeneracy. Hence, it becomes necessary to reexamine constraints posed from other cosmological considerations.

4.1. Structure Formation

It has been argued (Kang & Steigman 1992) that large neutrino degeneracy is ruled out from the implied delay in galaxy formation in such a hot dark matter universe. This argument is summarized (Kang & Steigman 1992) as follows:

Neutrino degeneracy speeds up the expansion rate by a factor

$$S_0^2(\xi_\nu) = 1 + 0.135(F(\xi_\nu) - 3) \approx 0.135F(\xi_\nu) , \quad (12)$$

where $F(\xi_\nu)$ is an effective energy density factor (Kang & Steigman 1992) for neutrinos.

For massless neutrinos we have from Equations 3 and 5,

$$F(\xi_\nu) = \sum_i F(\xi_{\nu_i}) = \sum_i \left(\frac{T_{\nu_i}}{T_\gamma} \right)_{Nuc}^4 \left[1 + \frac{15}{7} \left(\frac{\xi_{\nu_i}}{\pi} \right)^4 + \frac{30}{7} \left(\frac{\xi_{\nu_i}}{\pi} \right)^2 \right], \quad (13)$$

where $(T_{\nu_i}/T_\gamma)_{Nuc}$ is the neutrino-to-photon temperature ratio before e^\pm pair annihilation. This ratio is unity in the standard model with little or no degeneracy.

With the increased mass-energy in degenerate neutrinos, the time of matter-radiation equality occurs at smaller redshift and there is less time for the subsequent growth of fluctuations. The redshift $z_{eq}(\xi_\nu)$ for matter-radiation equality for a neutrino-degenerate universe can be written in terms of the redshift for a nondegenerate universe and the speed-up factor,

$$1 + z_{eq}(\xi_\nu) = S_0^{-2}(1 + z_{eq}(\xi_\nu = 0)), \quad (14)$$

For the present matter-dominated universe without neutrino degeneracy and $\Omega_M \leq 1$ we have $1 + z_{eq}(\xi_\nu = 0) \lesssim 1.06 \times 10^4$ (Kang & Steigman 1992). Furthermore, one demands that the fluctuation amplitude $A(z)$ grows at least linearly with redshift, i.e. $A(z) > (1 + z_{eq})A(z_{eq})$. One also requires that the amplitude at least reaches unity by the present time,

$$\frac{1}{A(z_{eq})} \lesssim (1 + z_{eq}) \lesssim \frac{A(z=0)}{A(z_{eq})}. \quad (15)$$

Thus, the requirement of sufficient growth in initial perturbations places a bound on the speed-up. Namely,

$$S_0^2 \lesssim \frac{1.06 \times 10^4}{1 + z_{eq}(\xi_\nu)} \lesssim 1.06 \times 10^4 A(z_{eq}). \quad (16)$$

Then requiring that $A(z_{eq}) \lesssim 10^{-3}$ (Steigman & Turner 1985) leads to the constraint that $F(\xi_\nu) \lesssim 10.6/.135 \approx 79$.

Figure 13 shows the $F(\xi_\nu)$ and $F(\xi_{\nu_i})$ calculated as a function of $\xi_{\nu_{\mu,\tau}}$ for the allowed models of Figure 8. Since our interesting parameter regions in Figure 8 satisfy $\xi_{\nu_e} \ll \xi_{\nu_{\mu,\tau}}$, only $\nu_{\mu,\tau}$ contribute significantly to the total $F(\xi_\nu)$. Also shown are values of $F(\xi_{\nu_i})$ if only one neutrino species was degenerate. The dashed line gives the constraint $F(\xi_\nu) \lesssim 79$ from Kang & Steigman (1992). For comparison, the two-dot dashed line also shows the $F(\xi_\nu)$ for a single species from Kang & Steigman (1992). For low values of $\xi_{\nu_{\mu,\tau}} \lesssim 4$, our $F(\xi_{\nu_i})$ values for a single degenerate species are nearly identical to those of Kang & Steigman (1992). However, as ξ_{ν_i} increases, our curves are lower due to the fact that we treat the annihilation epochs continuously (cf. Figure 4) rather than discretely, except for the QCD transition. By chance, our limit in the low degeneracy range for two degenerate neutrinos, ($\xi_{\nu_{\mu,\tau}} \lesssim 6.2$) is close to the single species limit ($\xi_i^{KS} \lesssim 6.9$) of Kang & Steigman (1992). In the present work, however, the single species limit for moderate degeneracy increases to $\xi_i \lesssim 8.2$.

Moreover, in the present work we now find that there also exists a new allowed region with $11.4 \lesssim \xi_{\nu_{\mu,\tau}} \lesssim 13$ for which this growth constraint is satisfied even for two degenerate species. For only one degenerate species the new allowed range expands to $11.4 \lesssim \xi_{\nu_{\mu}} \lesssim 16$. An upper limit of $\xi_{\nu_{\mu,\tau}} \lesssim 13$ for two degenerate neutrino species corresponds to allowed BBN models with a baryon fraction as large as $\Omega_b h_{50}^2 \lesssim 0.25$ (cf. Figure 8).

4.2. Neutrino Mass Constraint

Figure 12 summarizes the neutrino contribution to the closure density Ω_ν as a function of neutrino degeneracy and mass. This figure assumes the plausible model of nearly degenerate ν_μ and ν_τ masses and negligible ν_e mass. For this figure Ω_ν refers to the combined contributions from both ν_μ and ν_τ . The contribution changes for large degeneracy due to the lower present-day neutrino temperature. This figure can be used to constrain the masses of the ν and τ neutrino types in different cosmological models. For example, if we assume a model with $\Omega_b h_{50}^2 = 0.1$, $\Omega_\Lambda = 0.6$, and $\Omega_\nu = 0.3$, then we would find that the masses of both the ν_μ and ν_τ must be $\lesssim 2$ eV, if these two species are to provide the neutrino contribution to the closure density.

Studies of large scale structure also constrain neutrino masses and degeneracy in hot-dark-matter (HDM) and mixed-dark-matter (MDM) models. Indeed, at least some neutrino mass may presently be required to account for the observed power spectrum of galactic and microwave background structure. It has been argued (Primack et al. 1995) from considerations of structure formation in the early universe that two neutrino flavors (ν_μ, ν_τ) may have a rest mass of 2.4 eV, compatible with all neutrino oscillation experiments. This postulate solves the main problem of cold dark matter (CDM) models, i.e. production of too much structure on small scales. Furthermore, Larsen & Madsen (1995) argue that neutrino degeneracy is required in a MDM model with 2.4 eV neutrinos to obtain an optimum fit to the power spectrum. If we take 2.4 eV as the given mass of ν_μ and ν_τ , then for a $\Omega_\nu \lesssim 0.9$ $\Omega_b h_{50}^2 = 0.1$ MDM cosmology we would deduce from Figure 12 that the maximum degeneracy for two species with this mass would correspond to $\xi_{\nu_{\mu,\tau}} \lesssim 2.5$ similar to the values used in Larsen & Madsen (1995). We suggest that in light of the present results a similar study of the galactic power spectrum for $\xi_{\nu_{\mu,\tau}} \approx 11$ and $m_\nu \sim 0.1$ eV should be undertaken as well.

4.3. Cosmic Microwave Background Constraint

Perhaps, the most stringent remaining constraint on neutrino degeneracy comes from its effect on the cosmic microwave background. Several recent works (Kinney & Riotto 1999; Lesgourgues & Pastor 1999; Hannestad 2000) have shown that neutrino degeneracy can dramatically alter the power spectrum of the CMB. The essence of this constraint is that degenerate neutrinos increase the energy density in radiation at the time of photon decoupling in addition to delaying the time of matter-radiation energy-density equality as discussed above. One effect of this is to increase the amplitude of the first acoustic peak in the CMB power spectrum at $l \approx 200$. For example, based upon a χ^2 analysis (Lineweaver & Barbosa 1998) of 19 experimental points and window functions, Lesgourgues and Pastor (1999) concluded that $\xi_\nu \leq 6$ for a single degenerate neutrino species.

However, in the existing CMB constraint calculations (Kinney and Riotto 1999; Lesgourgues and Pastor 1999; Hannestad 2000) only small degeneracy parameters with the standard relic neutrino temperatures were utilized in their derived constraint. Hence, the possible effects of a diminished relic neutrino temperature for large neutrino degeneracy need to be reconsidered. To investigate this we have done calculations of the CMB power spectrum, $\Delta T^2 = l(l+1)C_l/2\pi$ based upon the CMBFAST code of Seljak & Zaldarriago (1996).

For the optimum neutrino-degenerate models ($\xi_{\nu_{\mu,\tau}} \approx 11$) and a neutrino contribution $\Omega_\nu \leq 0.25$ we deduce from the solid curve on Figure 9 that the neutrino mass is $m_{\nu_{\mu,\tau}} \leq 0.1$ eV and therefore unimportant during the photon decoupling epoch. Therefore, we only consider massless neutrinos here. For massless neutrinos it can be proven (Lesgourgues & Pastor 1999) that the only effect of neutrino degeneracy on the CMB is to increase the background pressure and energy density of relativistic particles (cf. Eqs. 1-3). We have in this way explicitly modified CMBFAST code to account for the contribution of massless degenerate neutrinos with a relic temperature ratio $y_\nu = T_\gamma/T_\nu$ as given in Figure 4.

We have evaluated χ^2 for fits to the CMB power spectrum, based upon the "radical compression" technique as described in Bond, Jaffe & Knox (2000). We have used the latest 69 observational points and window functions available from the web page given in that paper. The advantage of this approach is that the non-Gaussian experimental uncertainties in the power spectrum are correctly weighted in the evaluation of the goodness of fit.

For the purposes of the present study, we take as a benchmark the "All" case best fit $\Omega = 1$ model of Dodelson & Knox (2000) who derived cosmological parameters based upon this same data set and compression technique. Although there is some degeneracy in the cosmological parameters they deduced an optimum fit to the power spectrum for

$\Omega_b h^2 = 0.019$, $H_0 = 65 \text{ km sec}^{-1} \text{ Mpc}^{-1}$, $\Omega_\Lambda = 0.69$, $\Omega_M = 0.31$, $\tau = 0.17$, and $n = 1.12$, where Ω_M is the total matter contribution, τ is the reionization parameter, and n is the "tilt" of the power spectrum. This benchmark is plotted as the dashed curve in Figure 14. For this case we find $\chi^2 = 101$. [Note that our χ^2 is slightly different from that quoted in Dodelson & Knox (2000) because we use different binning of the power spectrum]. For comparison the "radical compression" of the CMB data into 14 bins used in this work is also shown (Bond et al. 2000).

Rather than to do an exhaustive parameter search we have taken an approach similar to Lesgourgues & Pastor (1999). That is, we fix several representative cosmological models and then study their goodness of fit to the CMB data. The best case for large neutrino degeneracy will be for a value of the degeneracy parameter $\xi_{\nu_{\mu,\tau}}$ such that neutrino decoupling occurs just before the QCD phase transition. This is the value for which the relic neutrino energy density is a local minimum (cf. Figure 13). For the present work this corresponds to $\xi_{\nu_{\mu,\tau}} = 11.4$, $\xi_{\nu_e} = 0.73$, $\Omega_b h_{50}^2 = 0.187$ models. In what follows we fix $\xi_{\nu_{\mu,\tau}}$, ξ_{ν_e} , and $\Omega_b h_{50}^2$ at these values and refer to this as the large degeneracy model.

We have found [as did Lesgourgues & Pastor (1999)] that the currently favored $\Omega_\Lambda = 0.7$ models give a poor fit to the data even with no degeneracy. Adding neutrino degeneracy to an $\Omega_\Lambda = 0.7$ model only makes the fit worse. The main problem is that the first acoustic peak increases in amplitude and moves to larger l . Hence, even though a local minimum develops for large degeneracy, the χ^2 is substantially increased and large neutrino degeneracy is probably ruled out for $\Omega_\Lambda = 0.7$ models.

For smaller Ω_Λ a local minimum develops in the χ^2 for both small values of degeneracy $\xi_{\nu_{\mu,\tau}} \approx 1$ and large degeneracy $\xi_{\nu_{\mu,\tau}} = 11.4$. As pointed out in Lesgourgues & Pastor (1999), the best case for neutrino degeneracy is with $\Omega_\Lambda = 0$ models. However, those models are probably ruled out by observations of type Ia supernovae at high redshift (Garnavich, et al. 1998; Perlmutter et al. 1998a; Perlmutter et al. 1998b; Riess et al. 1998). At the 3σ confidence level for $\Omega = 1$ models, the type Ia Supernova data are consistent with $\Omega_\Lambda = 0.7 \pm 0.3$. Hence, we take $\Omega_\Lambda = 0.4$ as a plausible cosmological model which is marginally consistent with the type Ia results. Nevertheless, for purposes of illustration, we have also made a search for optimum parameters for matter dominated $\Omega_\Lambda = 0$, $\Omega = 1$ models.

The reason low Ω_Λ models are favored is that they shift the first acoustic peak back to lower l . Larger values of H_0 also slightly improve the fit by shifting the first acoustic peak to lower l and decreasing the baryon density for fixed $\Omega_b h_{50}^2$ which lowers the peak amplitude. We take $H_0 = 65 \pm 10$ ($h_{50} = 1.3 \pm 0.2$) as a reasonable range (Dodelson & Knox 2000), and therefore utilize $h_{50} = 1.5$ as the optimum Hubble parameter for the

neutrino-degenerate models. This implies that $\Omega_b = 0.084$ for the large degeneracy models. The ionization parameter does not particularly help the fits as it mainly serves to decrease the amplitude of both the first and second peaks in the power spectrum. We therefore set $\tau = 0$ for the large degeneracy models. The only remaining adjustable parameter of the fits is then the tilt parameter n . Values of n slightly below unity also help with the amplitude and location of the first acoustic peak.

The solid line on Figure 14 shows a $\Omega_\Lambda = 0.4$ model for which $n = 0.78$. For this fit $\Delta\chi^2 = 27$ which makes this large degeneracy model marginally consistent with the data at a level of 5.2σ . The dotted line in Figure 14 shows the matter dominated $\Omega_\Lambda = 0$ best fit model with $n = 0.83$. For this fit $\Delta\chi^2 = 9$ which makes this large degeneracy model consistent with the data at the level of 3σ .

As can be seen from Figure 14, a model with large neutrino degeneracy seems marginally acceptable based upon the presently uncertain power spectrum. The main differences in the fits between the large degeneracy models and our adopted benchmark model are that the first peak is shifted to slightly higher l values and the second peak is somewhat suppressed. It thus becomes important to quantify the amplitude of the second peak in order to constrain the large degeneracy models proposed herein.

Indeed, after the present fits were completed a suppression of the second acoustic peak in the power spectrum was reported in the high-resolution BOOMERANG (Bernardls, P. et al. 2000; Lange et al. 2000) and MAXIMA-1 (Hanany et al. 2000; Balbi et al. 2000) results. We have not yet analyzed the goodness of fit to these data as the experimental window functions are not yet available. In a subsequent paper we will examine the implications of those data in detail.

For purposes of illustration, however, we compare the fit models of Figure 14 with the published BOOMERANG and MAXIMA-1 power spectra in Figure 15. Here one can clearly see that the suppression of the second acoustic peak in the observed power spectrum is consistent with our derived neutrino-degenerate models. In particular, the MAXIMA-1 results are in very good agreement with the predictions of the neutrino-degenerate cosmological models described herein. There is, however, a calibration uncertainty between these two sets (Hanany et al. 2000). If one only considers the BOOMERANG results alone, the diminished amplitude of the first acoustic peak probably tightens the constraint for low neutrino degeneracy models (cf. Hannestad 2000) although even for this set alone, a high degeneracy model is probably still acceptable (Lesgourgues & Peloso 2000). It is clear, that these new data sets will substantially improve the goodness of fit for the neutrino-degenerate models (Lesgourgues & Peloso 2000). Moreover, both data sets seem to require an increase in the baryonic contribution to the closure density as allowed in our

neutrino-degenerate models.

5. CONCLUSIONS

We have discussed how the relic neutrino temperature is substantially diminished in cosmological models with a large neutrino degeneracy. We have shown that all of the BBN light-element abundance constraints (assuming some destruction of ${}^7\text{Li}$) can be satisfied for a single-parameter family of cosmological models in which significant neutrino degeneracies and large values of $\Omega_b h^2$ can exist. The requirement that large scale structure become nonlinear in sufficient time can also be satisfied for models with either moderate degeneracy ($\xi_{\nu_{\mu,\tau}} \lesssim 6.2$ and $\Omega_b h_{50}^2 \lesssim 0.22$) or large neutrino degeneracy ($11.4 \lesssim \xi_{\nu_{\mu,\tau}} \lesssim 13$ and $0.187 \lesssim \Omega_b h_{50}^2 \lesssim 0.25$). We have also shown that even the constraint from neutrino-degeneracy effects on fluctuations of the cosmic microwave background temperature may be marginally avoided for models with $\Omega_\Lambda \lesssim 0.4$, $\xi_{\nu_{\mu,\tau}} \approx 11$, and $\Omega_b h_{50}^2 \approx 0.2$.

At present, the power spectrum of the CMB is the most stringent constraint. Nevertheless, neutrino-degenerate models can be found which are marginally consistent at the 3-5 σ level. This tight constraint is due, at least in part, to a suppression of the second acoustic peak in the spectrum. It is therefore encouraging that the recent BOOMERANG and MAXIMA-1 results suggest that such a suppression in the second acoustic peak may indeed occur in agreement with the expectations of the large neutrino degeneracy, high Ω_b models proposed here.

Thus, high resolution microwave background observations become even more important as a means to quantify the limits to (or existence of) possible cosmological neutrino degeneracy. Based upon the current analysis, we conclude that all of the cosmological constraints on large neutrino degeneracy are marginally satisfied when a careful accounting of the neutrino decoupling and relic neutrino temperature is made. It will, therefore, be most interesting to see what further constraints can be placed on this possibility from the soon to be available space-based high resolution CMB observations such as the NASA MAP and ESA Planck missions.

One of the authors (GJM) wishes to acknowledge the hospitality of the National Astronomical Observatory of Japan where much of this work was done. This work has been supported in part by the Grant-in-Aid for Scientific Research (10640236, 10044103, 11127220, 12047233) of the Ministry of Education, Science, Sports, and Culture of Japan, and also in part by NSF Grant (PHY-9901241 at OSU) along with DoE Nuclear Theory

Grant (DE-FG02-95-ER40394 at UND).

REFERENCES

- Affleck, I., & Dine, M. 1985, Nucl. Phys. B., **249**, 361
- Angulo, C. et al. (NACRE collaboration) 1999, Nucl. Phys. A., **656**, 3
- Bahcall, N. A., Lubin, L. M., & Dorman, V. 1995, ApJ, **447**, L81
- Balbi, A. et al. 2000, ApJ, **545**, L1
- Bell, N. F., Foot, R., & Volkas, R. R., 1998, Phys. Rev. D., **58**, 105010
- Beaudet, G., & Goret, P. 1976, A&A, **49**, 415
- Beaudet, G., & Yahil, A. 1977, ApJ, **218**, 253
- Bernardls, P. et al. (Boomerang Collaboration) 2000, Nature., **404**, 955
- Bond, J. R., Jaffe, A. H. & Knox, L. 2000, ApJ, **533**, 19; Dataavailable from:
<http://www.cita.utoronto.ca/knox/radical.html>
- Burles, S. & Tytler, D. 1998a, ApJ, **499**, 699
- Burles, S. & Tytler, D. 1998b, ApJ, **507**, 732
- Casas, A., Cheng, W. Y., & Gelmini, G. 1999, Nucl. Phys. B., **538**, 297
- Copi, C. J., Schramm, D. N., & Turner, M. S. Science 1995 **267** 192; 1995, ApJ, **455**, L95
- David, Y., & Reeves, H. 1980, Phil. Trans. Roy. Soc., **A296**, 415
- David, L. P., Jones, C. J., & Forman, W. 1995, ApJ, **445**, 578
- Dodelson, S. & Knox, L. 2000, Phys. Rev. Lett., **84**, 3523
- Dolgov, A. & Kirilova, D. P. J. 1991, Moscow Phys. Soc., **1**, 217
- Dolgov, A. 1992, Phys. Rep., **222**, 309
- Enqvist, K., Kainulainen, K., & Semikoz, V. 1992, Nucl. Phys. B., **374**, 392
- Esposito, S., Mangano, G., Miele, G., & Pisanti, O. 1999, Nucl. Phys. B., **540**, 3

- Freese, K., Kolb, E. J., & Turner, M. S., 1983, Phys. Rev. D., **27**, 1689
- Fornengo, N., Kim, C. W., & Song, J., 1997, Phys. Rev. D., **56**, 5123
- Fry, J. N., & Hogan, C. J. 1982, Phys. Rev. Lett., **49**, 1873
- Garnavich, P. M. et al. 1998, ApJ, **509**, 74
- Gelmini, G. & Kusenko, A. 1999, Phys. Rev. Lett., **82**, 5202
- Gondolo, P., & Gelmini. G. 1991, Nucl. Phys. B., **360**, 145
- Greisen, K. 1966, Phys. Rev. Lett., **16**, 748
- Hannestad, S. 2000, Phys. Rev. Lett., **85**, 4203
- Hanany, S. et al. (MAXIMA-1 Collaboration) 2000, ApJ, **545**, L5
- Harvey, J. A. & Kolb, E. W. 1981, Phys. Rev. D., **24**, 2090
- Hata, N., Scherrer, R. J., Steigman, G., Thomas, D. & Walker, T. P. 1996, ApJ, **458**, 637
- Herndl, H., Hofinger, R., Jank, J., & Oberhummer, H., Görres, J., Wiescher, M., Thielemann, F. K., Brown, B. A. 1999, Phys. Rev. C., **60**, 064614
- Kajino, T. & Orito, M. 1998, Nucl. Phys. A., **629**, 538c
- Kajino, T. & Orito, M. 1998, in "Nuclei in the Cosmos V, Proc. 5th International Conference, Volos, Greece, July 6-12, (Editions Frontieres; France), N. Prantzos, ed. pp. 17-20.
- Kajino, T., Suzuki, T.-K., Kawanomoto, S., & Ando, H. 2000, in *The Light Elements and Their Evolution*, IAU Symposium Vol 198, L. Da Silva, M. Spite and J. R. de Mederras, eds. (in press).
- Kang, H., & Steigman, G. 1992, Nucl. Phys. B., **372**, 494
- Kim, J. B., & Lee, H. K. 1995, ApJ, **448**, 510
- Kim, J. B., Kim J. H., & Lee, H. K. 1998, Phys. Rev. D., **58**, 027301
- Kinney, W. K. & Riotto, A. 1999, Phys. Rev. Lett., **83**, 3366
- Kohri, K., Kawasaki, M., & Sato, K. 1997, ApJ, **490**, 72
- Larsen, G. B., and Madsen, J. 1995, Phys. Rev. D., **52**, 4282

- Lange, A. E. et al. 2000, preprint, astro-ph/0005004
- Levshakov, S. A., Tytler, D., & Burles, S. 1999, AJ submitted., Los Alamos e-Print Archive., astro-ph/9812114
- Lesgourgues, J., Polarski, D. & Starobinsky, A. A. 1999, MNRAS, **308**, 281
- Lesgourgues, J., Peloso, M. 2000, Phys. Rev. D., **62**, 081301
- Lesgourgues, J. & Pastor, S. 1999, Phys. Rev. D., **60**, 103521
- Lineweaver, C. H. & Barbosa, D. 1998, A&A, **319**, 799;1998, ApJ, **496**, 624
- Lopez, R. E., & Turner, M. S. 1999, Phys. Rev. D., **59**, 103502
- Lyttleton, R. A., & Bondi, H., 1959, Proc. R. Soc. London. **A252**, 313
- Mohr, P., Herndl, H., & Oberhummer, H. 1999 preprint.
- Nolett, K. M., & Burles, S. 2000, Phys. Rev. D., **61**, 123505
- Olive, K. A., Schramm, D. N., Thomas, D., & Walker, T. P. 1991, Phys. Lett. B., **265**, 239
- Olive, K. A. & Steigman, G. 1995, ApJS, **97**, 49
- Olive, K. A., Steigman, G., & Skillman, E. D. 1997, ApJ, **483**, 788
- Olive, K. A., Steigman, G., & Walker, T. P. 2000, Phys. Rep., **333-334**, 389
- Orito, M., Kajino, T., & Oberhummer, H. 1998, in "Nuclei in the Cosmos V, Proc. 5th International Conference, Volos, Greece, July 6-12, (Editions Frontieres; France), N. Prantzos, ed. pp. 37-40
- Perlmutter, S. et al. 1998a, Nature., **391**, 51
- Perlmutter, S. et al. 1998b, ApJ, **517**, 565
- Piembert, M. & Piembert, A. 2000, in *The Light Elements and Their Evolution*, IAU Symposium Vol 198, L. Da Silva, M. Spite and J. R. de Mederras, eds. (in press).
- Primack, J. R., Holtzman, J., Klypin, A., and Caldwell, D. O., 1995, Phys. Rev. Lett., **74**, 2160
- Riess, A. G. et al. 1998, AJ, 116, 1009
- Ryan, S. G., Beers, T. C., Olive, K. A., Fields, B. D., & Norris, J. E., 1999, ApJ, **530**, L57

- Scherrer, R. J. 1983 MNRAS, **205**, 683
- Schramm, D. N. & Mathews, G. J. 1995, in Nuclear and Particle Astrophysics in the Next Millennium, ed. E. Kolb, et al. (Singapore: World Scientific), pp. 479-497.
- Seljak, U. & Zaldarriago, M. 1996, ApJ, **469**, 437
- Smith, M. S., Kawano, L. H. & Malaney, R. A., 1993, ApJS, **85**, 219
- Starkman, G. D. 1992, Phys. Rev. D., **45**, 476
- Steigman, G. 2000, astro-ph/0002296, in *The Light Elements and Their Evolution*, IAU Symposium Vol 198, L. Da Silva, M. Spite and J. R. de Mederras, eds. (in press).
- Steigman, G. & Turner, M.S. 1985, Nucl. Phys. B., **253**, 375
- Steigman, G., 1996, Nucl. Phys. Proc. Suppl. **48** 499.
- Terasawa, N., & Sato, K. 1985, ApJ, **29**, 9
- Terasawa, N., & Sato, K. 1988, Prog. Theor. Phys., **80** 468
- Tytler, D., O’Meara, J. M., Suzuki, N., & Lubin, D. 2000, astro-ph/0001318, to appear in Physica Scripta
- Wagemans, J., Wagemans, C., Bieber, R., & Geltenbort, P. 2000, Phys. Rev. C., **61**, 064601
- Wagoner, R. V., Fowler, W.A., & Hoyle, F. 1967, ApJ, **148**, 3
- Walker, T. P., Steigman, G., Schramm, D. N., Olive, K. A., & Kang, H. 1991, ApJ, **376**, 51
- White, S. D. M., Navarro, J. F., Evrard, A. E. & Frenk, C. S. 1993, Nature., **366**, 429.
- White, D. A., Fabian, A. C. 1995, MNRAS, **273**, 72
- Yahil, A., & Beaudet, G. 1976, ApJ, **206**, 26

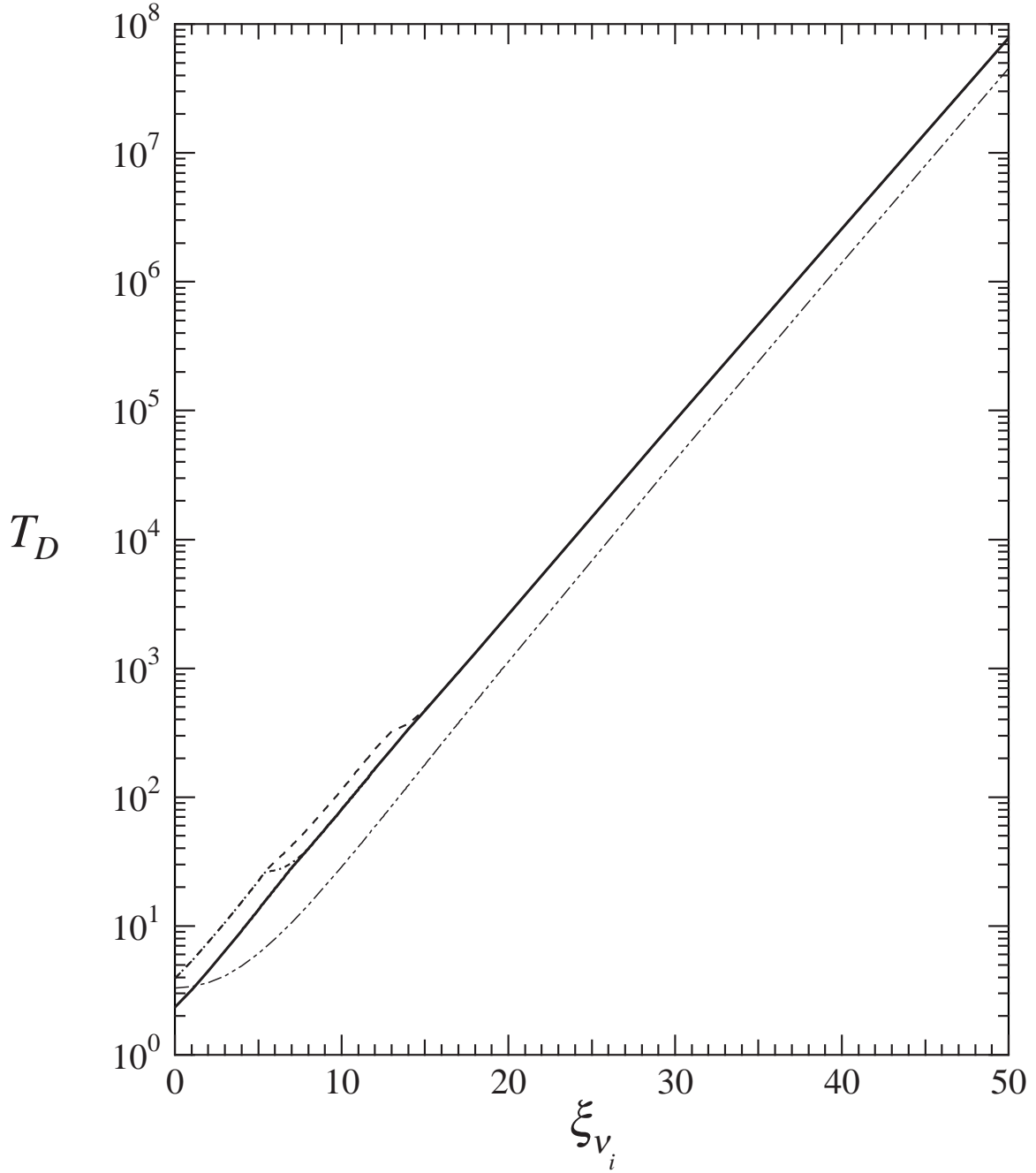


Fig. 1.— Decoupling temperature T_D (in MeV) for ν_e (solid line), ν_μ (dot-dashed line), and ν_τ (dashed line) as a function of degeneracy parameter ξ_{ν_i} , compared with the previous estimate (two-dot dashed line) of Kang & Steigman (1992)

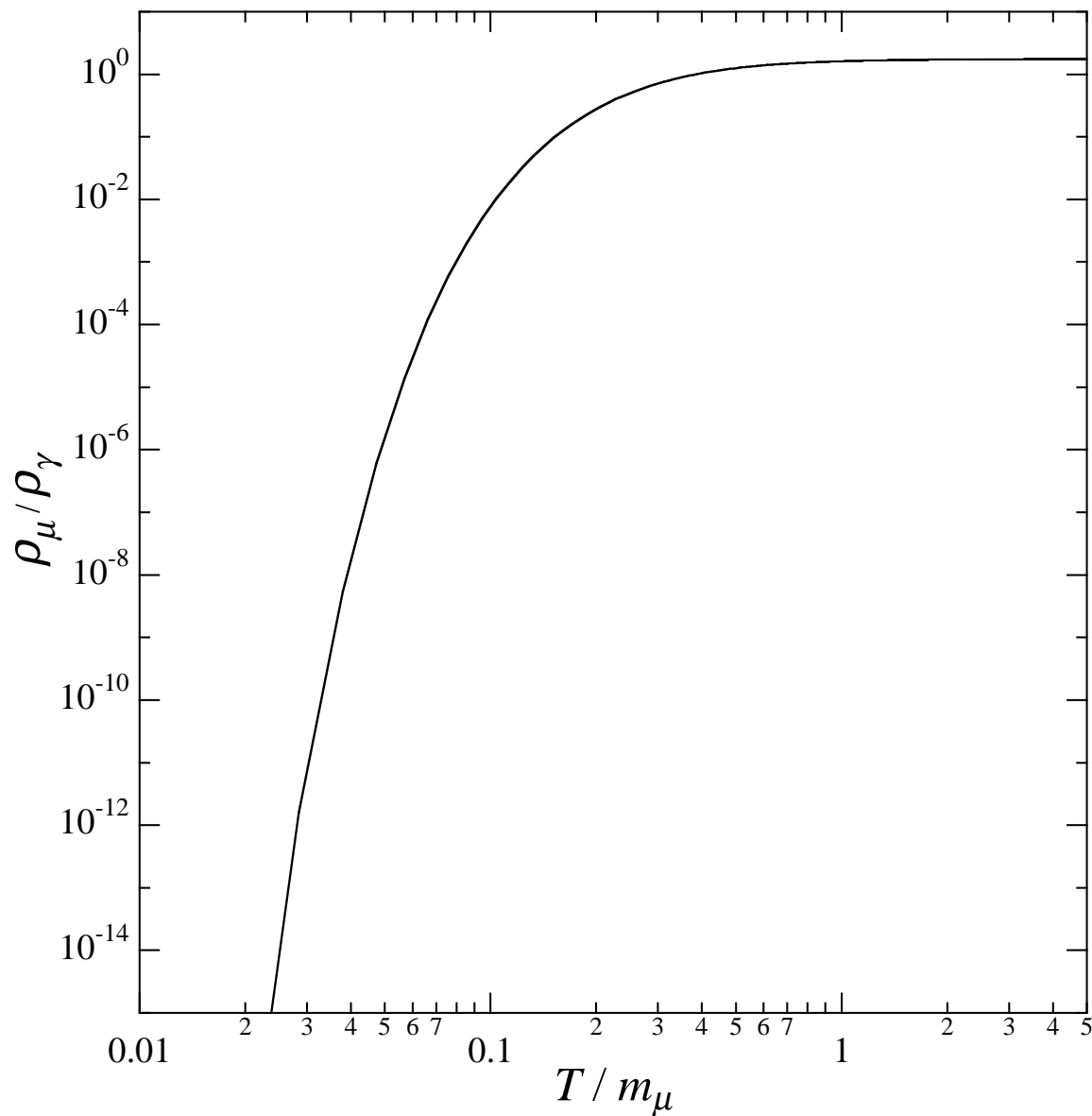


Fig. 2.— Ratio of the energy density of muons (or any massive particle μ) to photons as a function of the ratio of temperature to rest mass. This shows that even at a temperature of only $\sim 20\%$ of the rest mass, a significant fraction ($\sim 10\%$) of the energy density still resides in particle/antiparticle pairs.

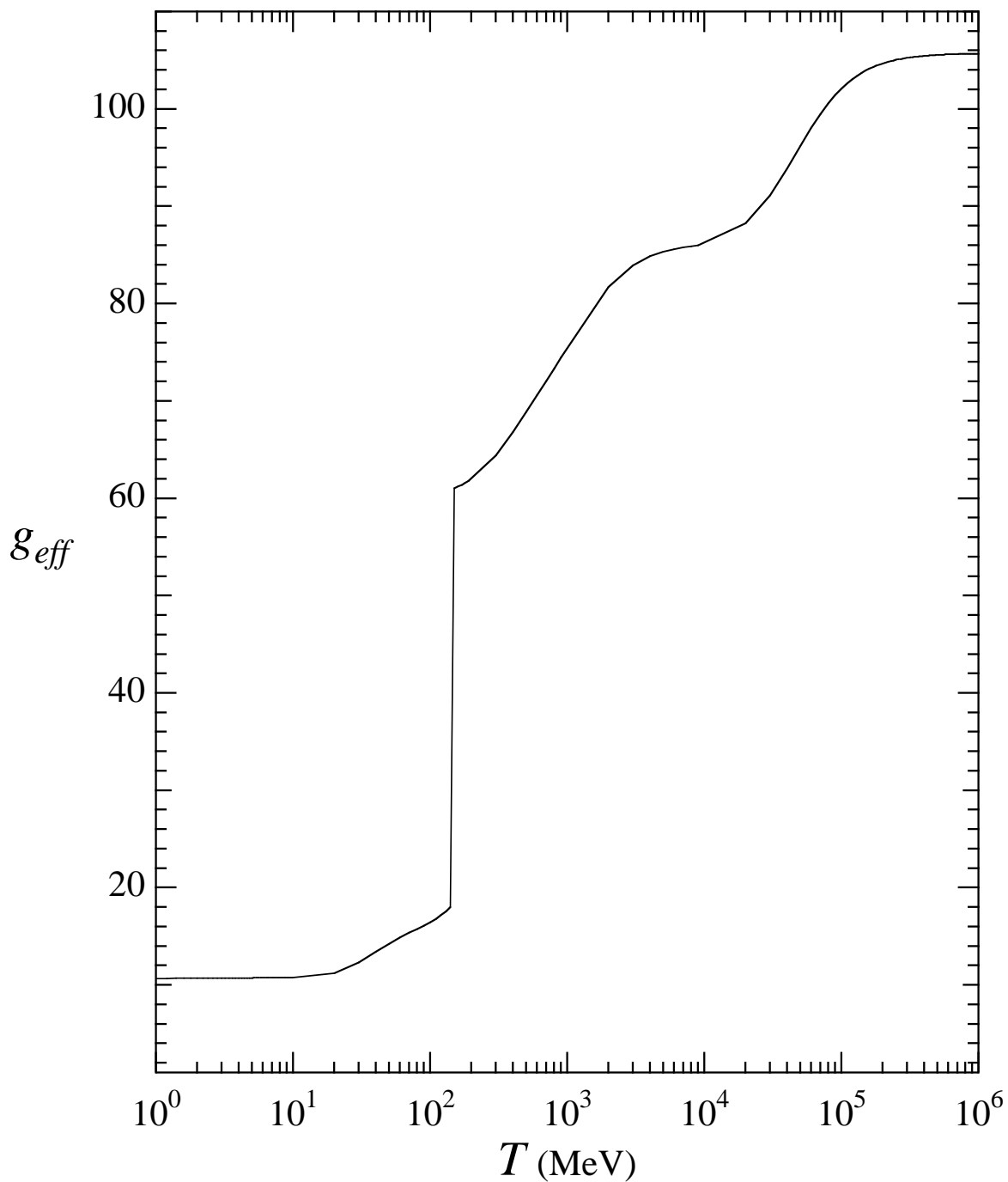


Fig. 3.— An illustration of the effective degrees of freedom g_{eff} as a function of temperature for a standard big bang with 3 nondegenerate neutrinos. For this illustration we have assumed that the neutrinos do not decouple until $T \approx \text{MeV}$. The discontinuity at $T = 150$ MeV is due to the QCD phase transition.

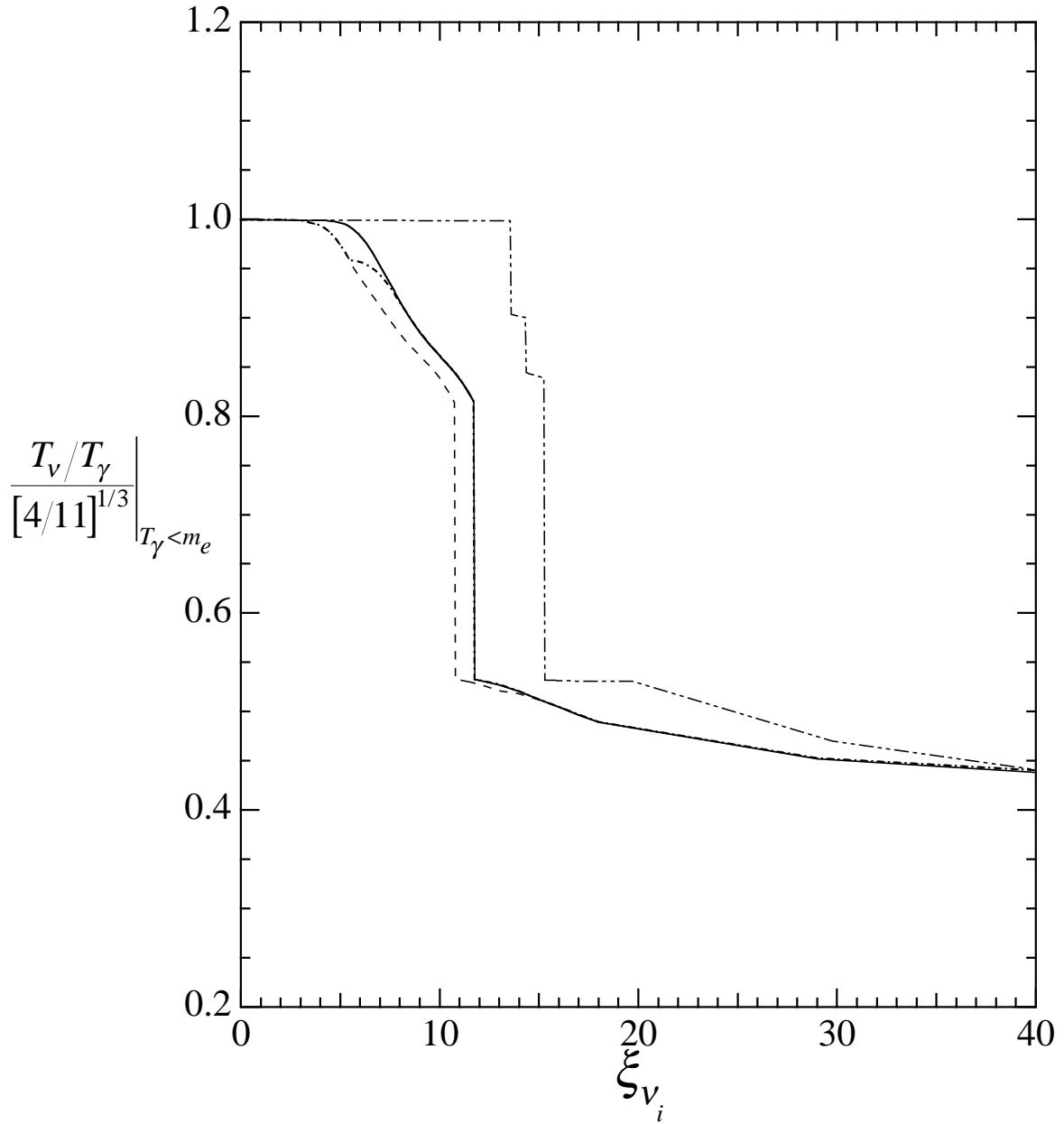


Fig. 4.— Ratio of relic neutrino temperature to photon temperature as a function of degeneracy parameter for each neutrino species for ν_e (solid line), ν_μ (dot-dashed line), ν_τ (dashed line), compared with the previous estimate (two-dot dashed line) of Kang & Steigman (1992)

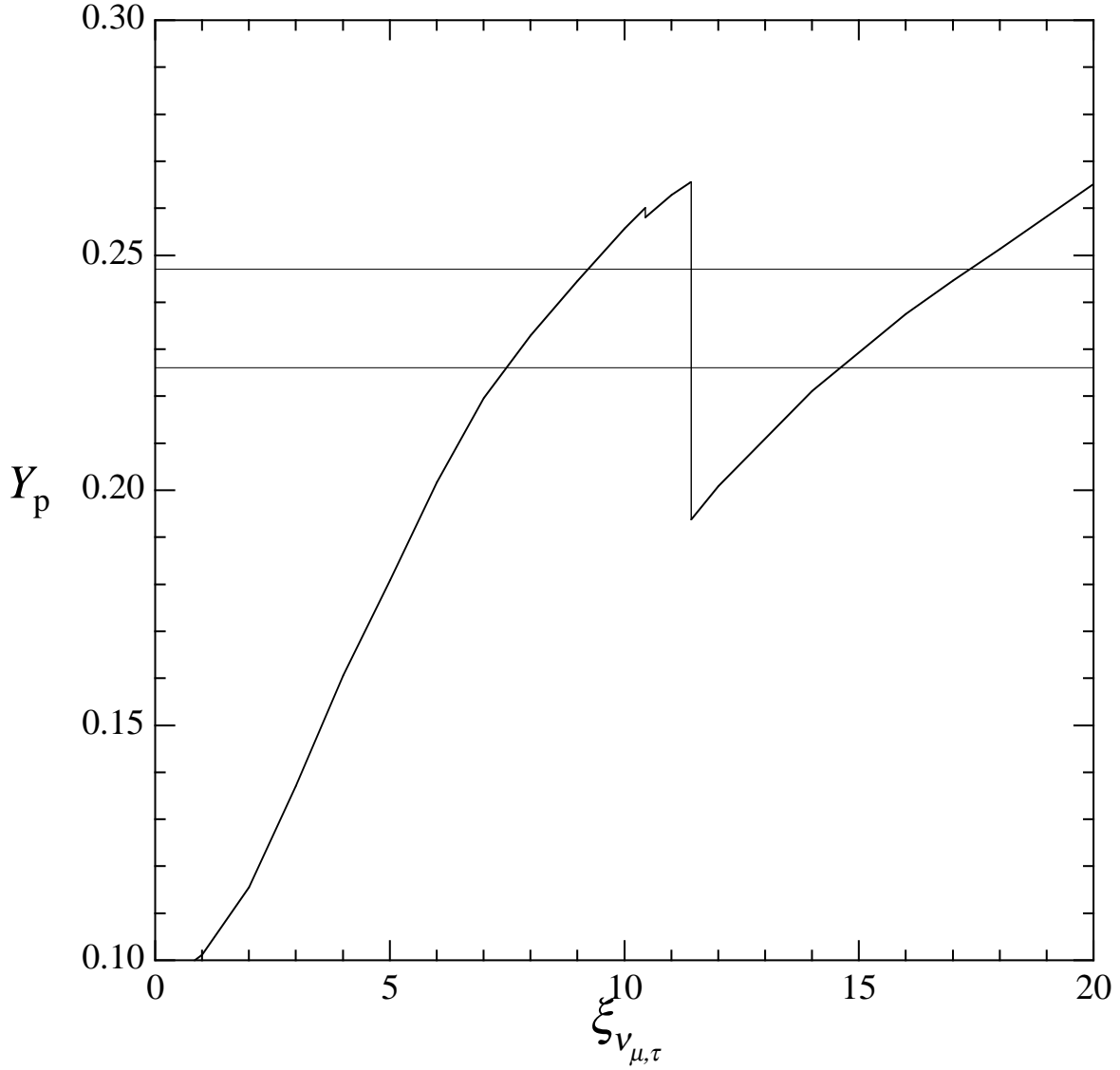


Fig. 5.— Helium mass fraction Y_p as a function of degeneracy parameter $\xi_{\nu_{\mu,\tau}}$ for $\Omega_b h_{50}^2 = 0.3$ and $\xi_{\nu_e} = 0.9$. Horizontal lines show the adopted observational constraints.

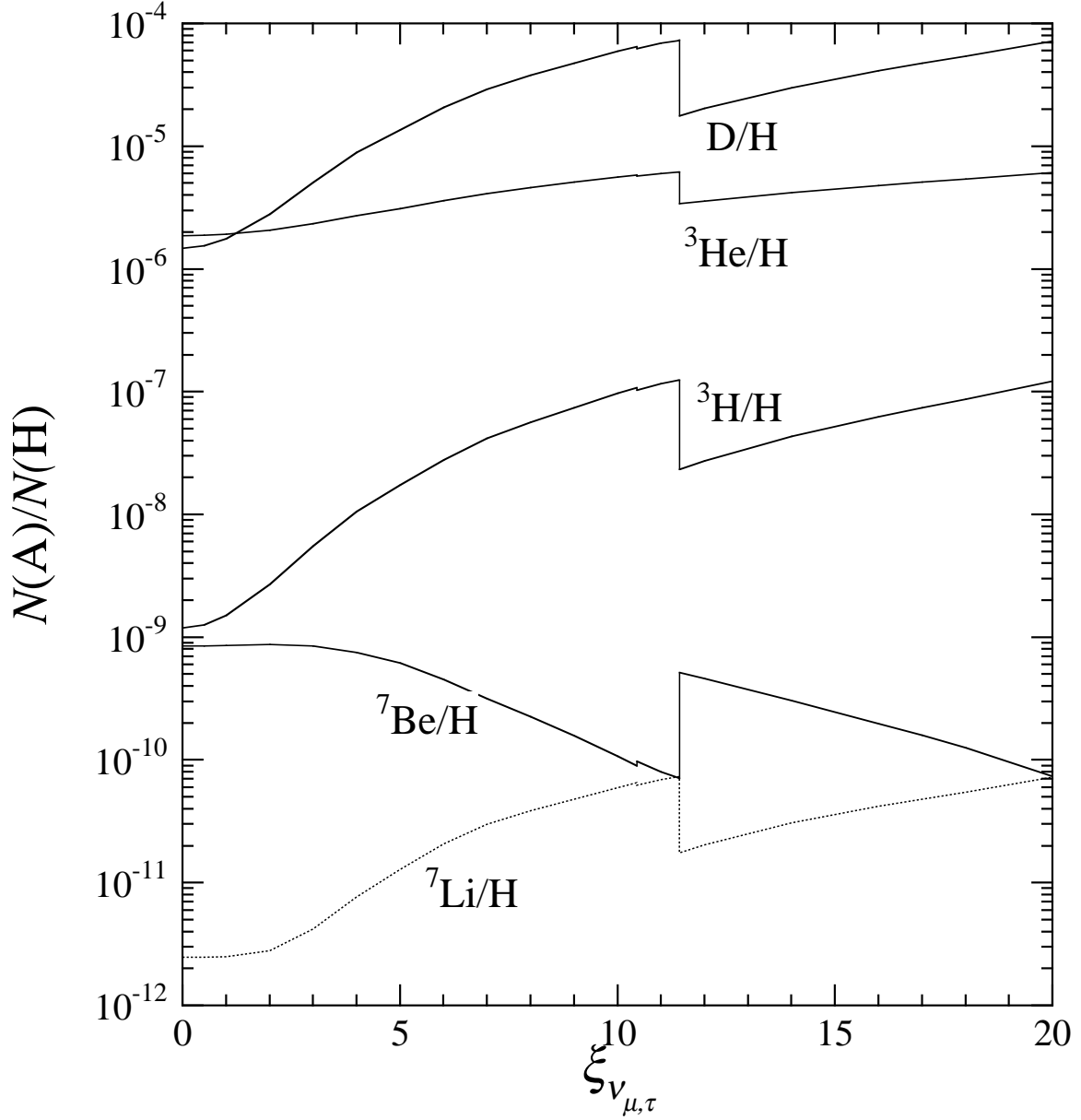


Fig. 6.— The predicted abundances of the light elements as a function of the neutrino degeneracy $\xi_{\nu_{\mu,\tau}}$ for $\Omega_b h_{50}^2 = 0.3$ and $\xi_{\nu_e} = 0.9$.

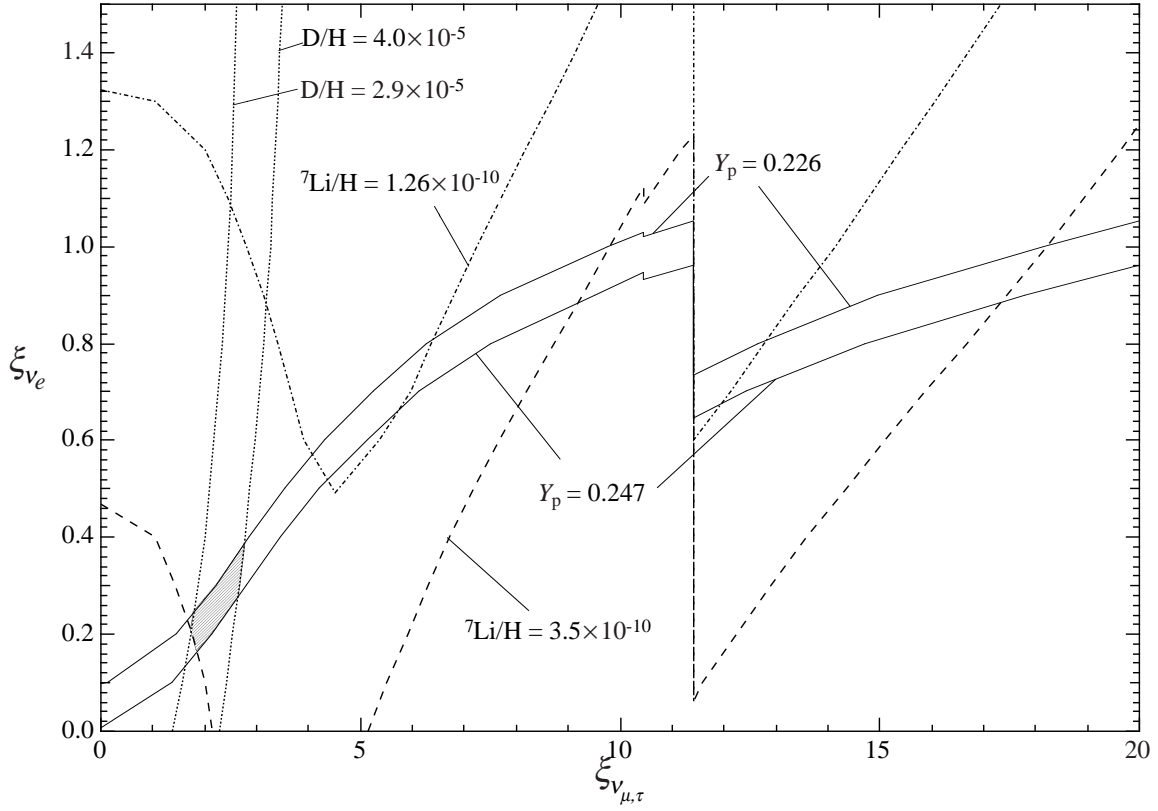


Fig. 7(a).— Contours of allowed values in the ξ_{ν_e} - $\xi_{\nu_{\mu,\tau}}$ plane for $\Omega_b h_{50}^2 = 0.1$, based upon the various light-element abundance constraints as indicated. The hatched region depicts the allowed parameters consistent with all light element constraints for this value of $\Omega_b h_{50}^2$.

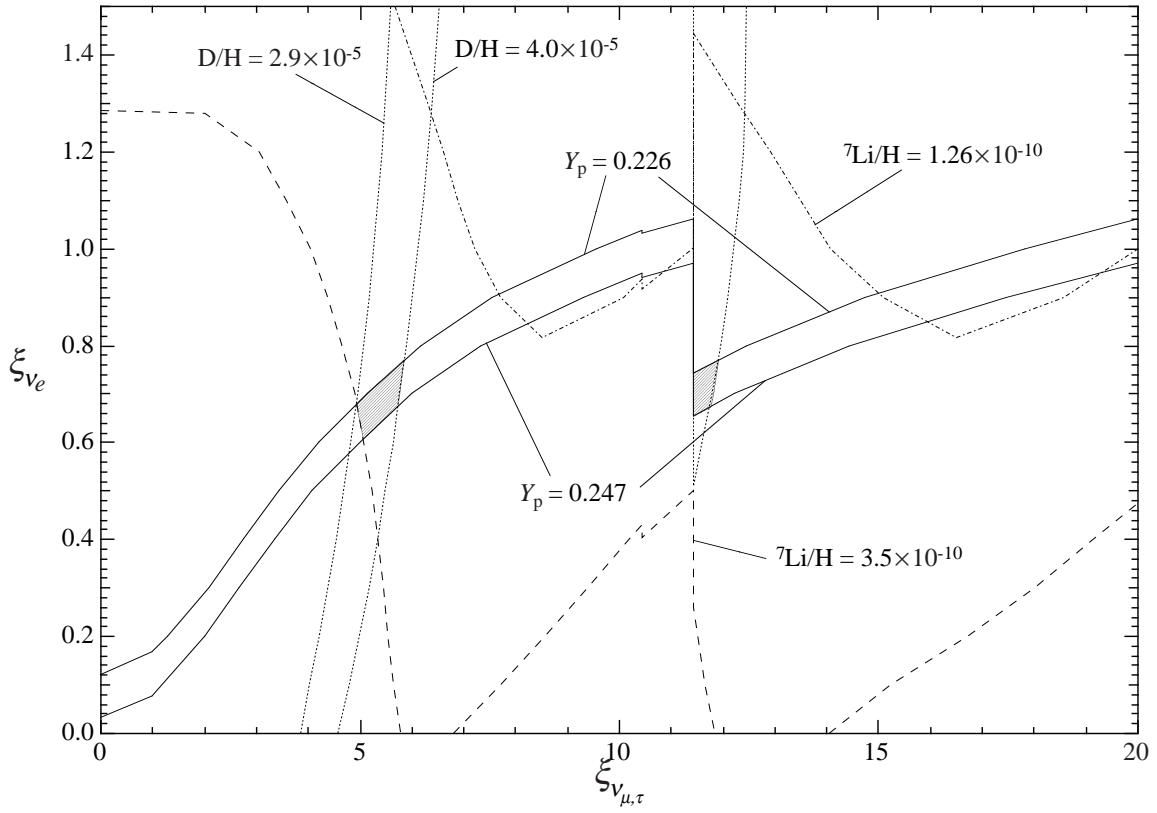


Fig. 7(b).— Same as Fig7a, but for $\Omega_b h_{50}^2 = 0.2$.

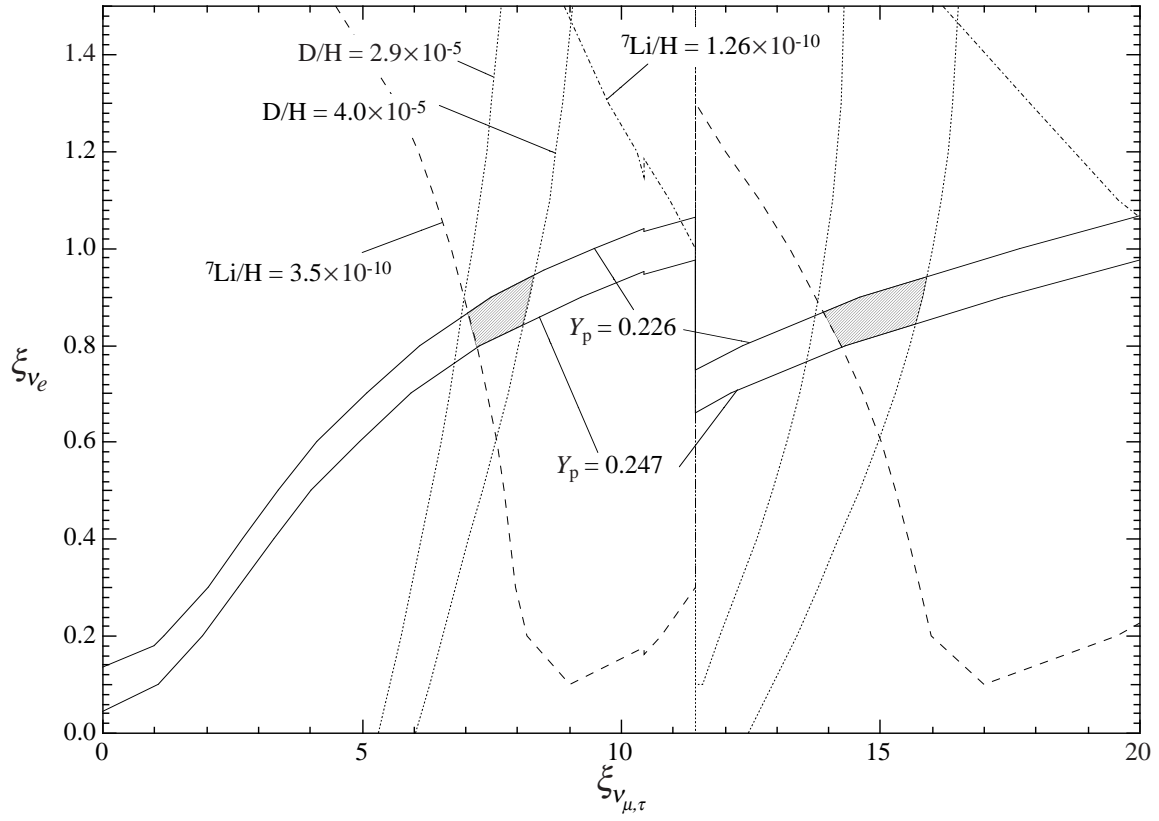


Fig. 7(c).— Same as Fig7a, but for $\Omega_b h_{50}^2 = 0.3$.

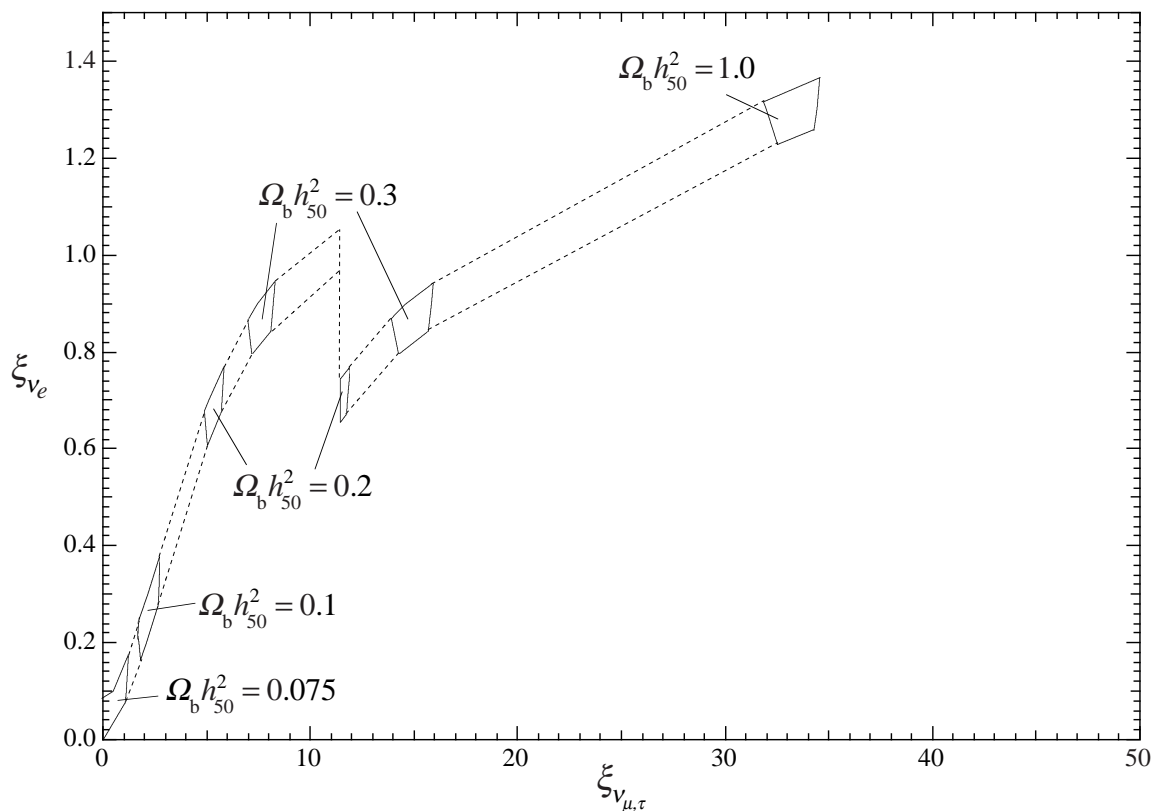


Fig. 8.— Allowed values of ξ_{ν_e} and $\xi_{\nu_{\mu,\tau}}$ for which the constraints from light element abundances are satisfied for values of $\Omega_b h_{50}^2 = 0.075, 0.1, 0.2, 0.3$ and 1.0 as indicated. For large values of $\Omega_b h_{50}^2 > 0.3$ the only allowed regions are for the large values $\xi_{\nu_{\mu,\tau}} > 20$.

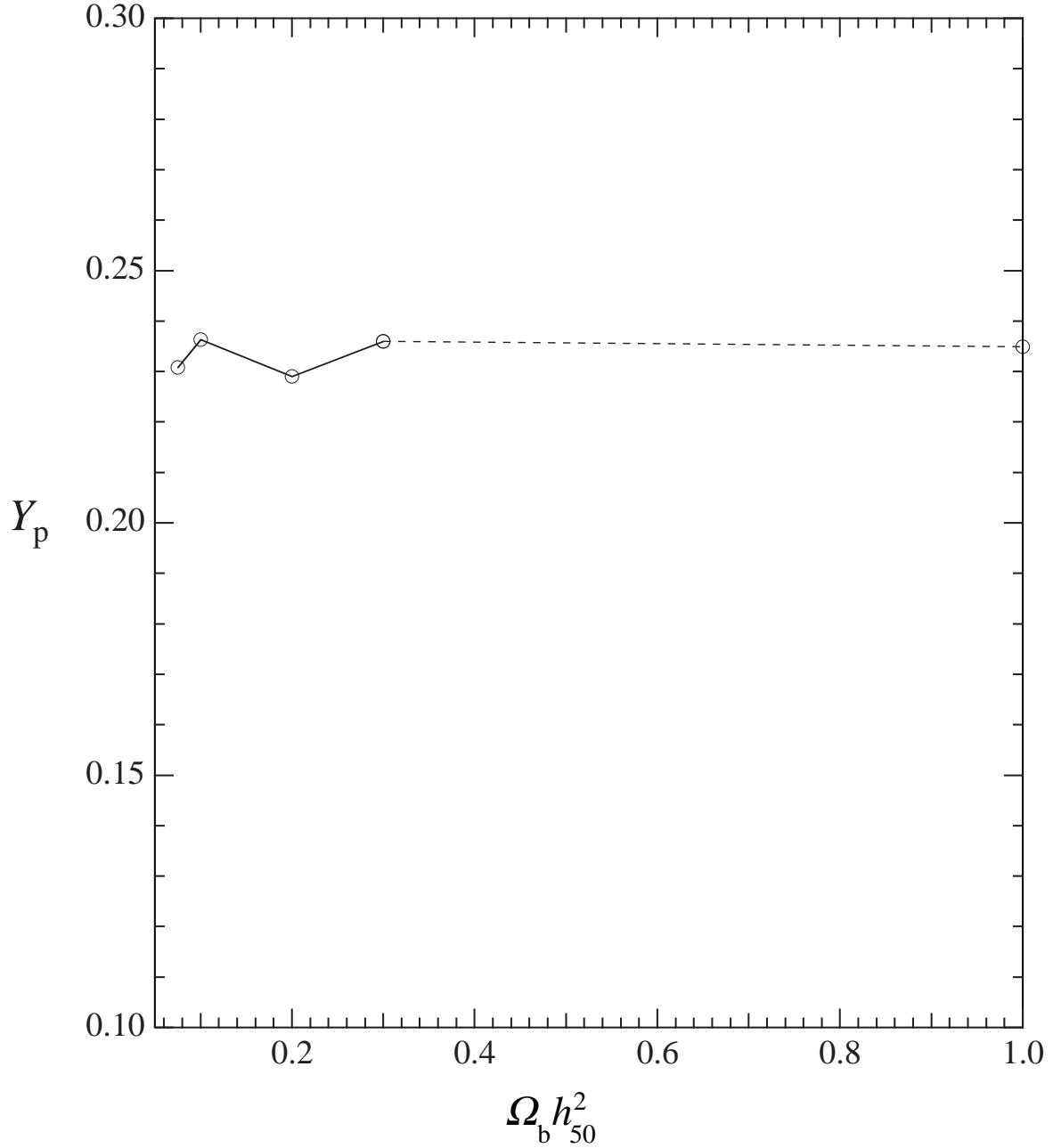


Fig. 9.— The predicted Helium abundance for allowed neutrino-degenerate models as a function of $\Omega_b h_{50}^2$. The values of ξ_{ν_e} and $\xi_{\nu_{\mu,\tau}}$ were taken from the central value in the allowed region determined by $\Omega_b h_{50}^2$ in Fig. 8. Note that Y_p is sensitive to the choice of ξ_{ν_e} in the allowed region.

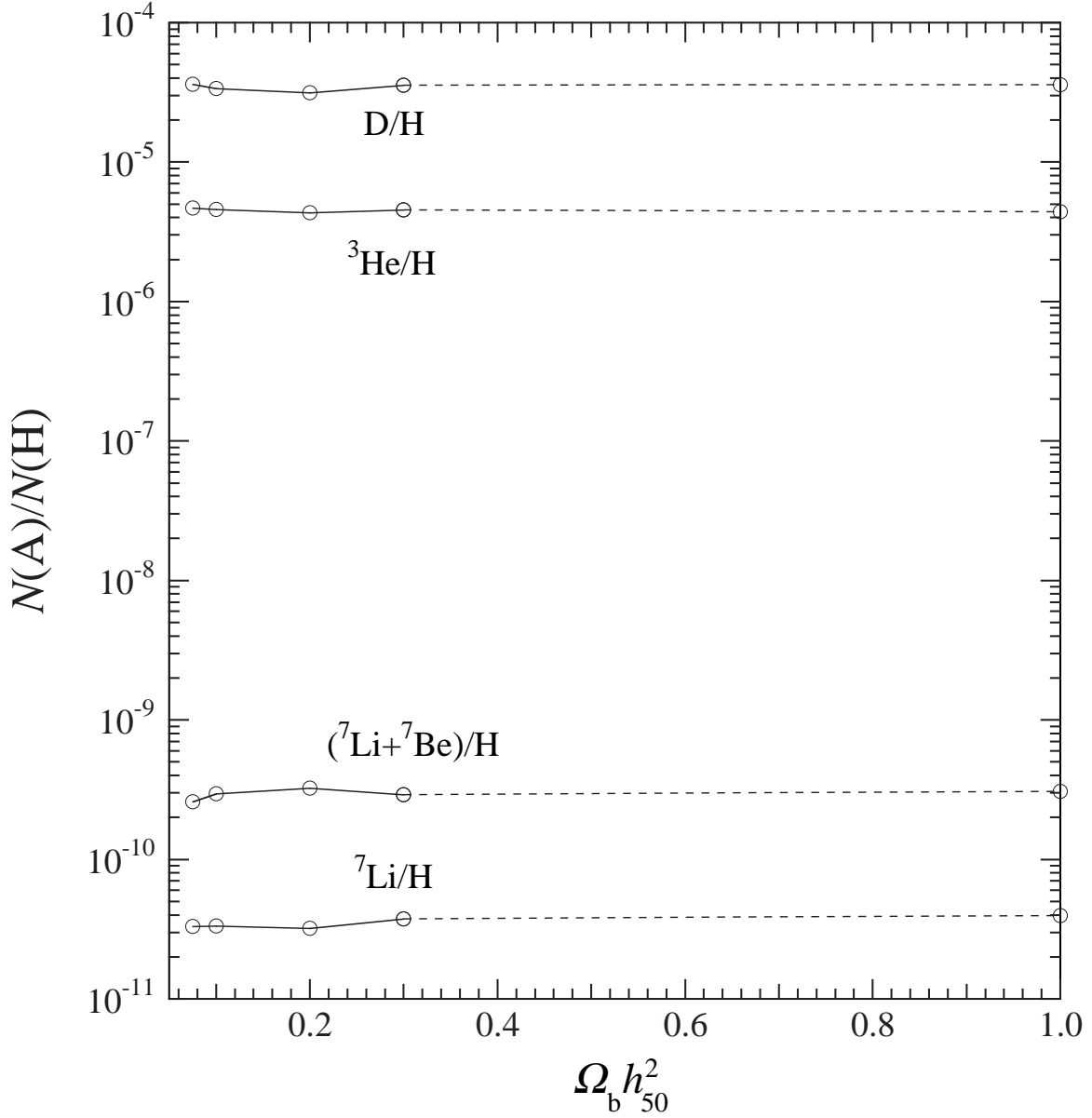


Fig. 10.— The predicted D/H, ${}^3\text{He}/\text{H}$, and total $A = 7$ and ${}^7\text{Li}$ abundances for allowed neutrino-degenerate models as a function of $\Omega_b h_{50}^2$. The values of ξ_{ν_e} and $\xi_{\nu_{\mu,\tau}}$ were taken from the central value in the allowed region determined by $\Omega_b h_{50}^2$ in Fig. 8.

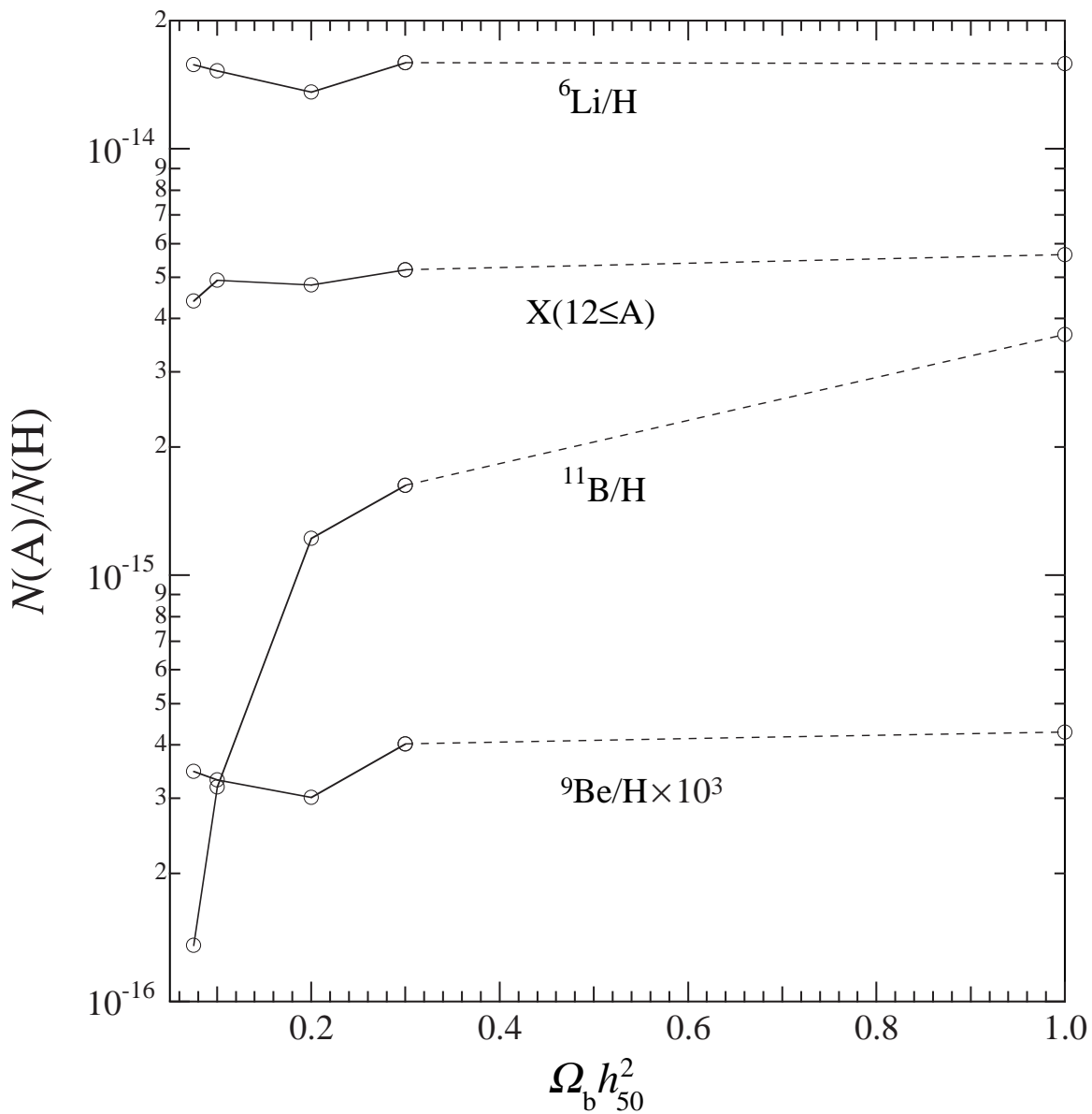


Fig. 11.— The predicted ${}^6\text{Li}$, ${}^9\text{Be}$, ${}^{11}\text{B}$ and $A \geq 12$ heavier element abundances as a function of $\Omega_b h_{50}^2$. The values of ξ_{ν_e} and $\xi_{\nu_{\mu,\tau}}$ were taken from the central value in the allowed region determined by $\Omega_b h_{50}^2$ in Fig. 8.

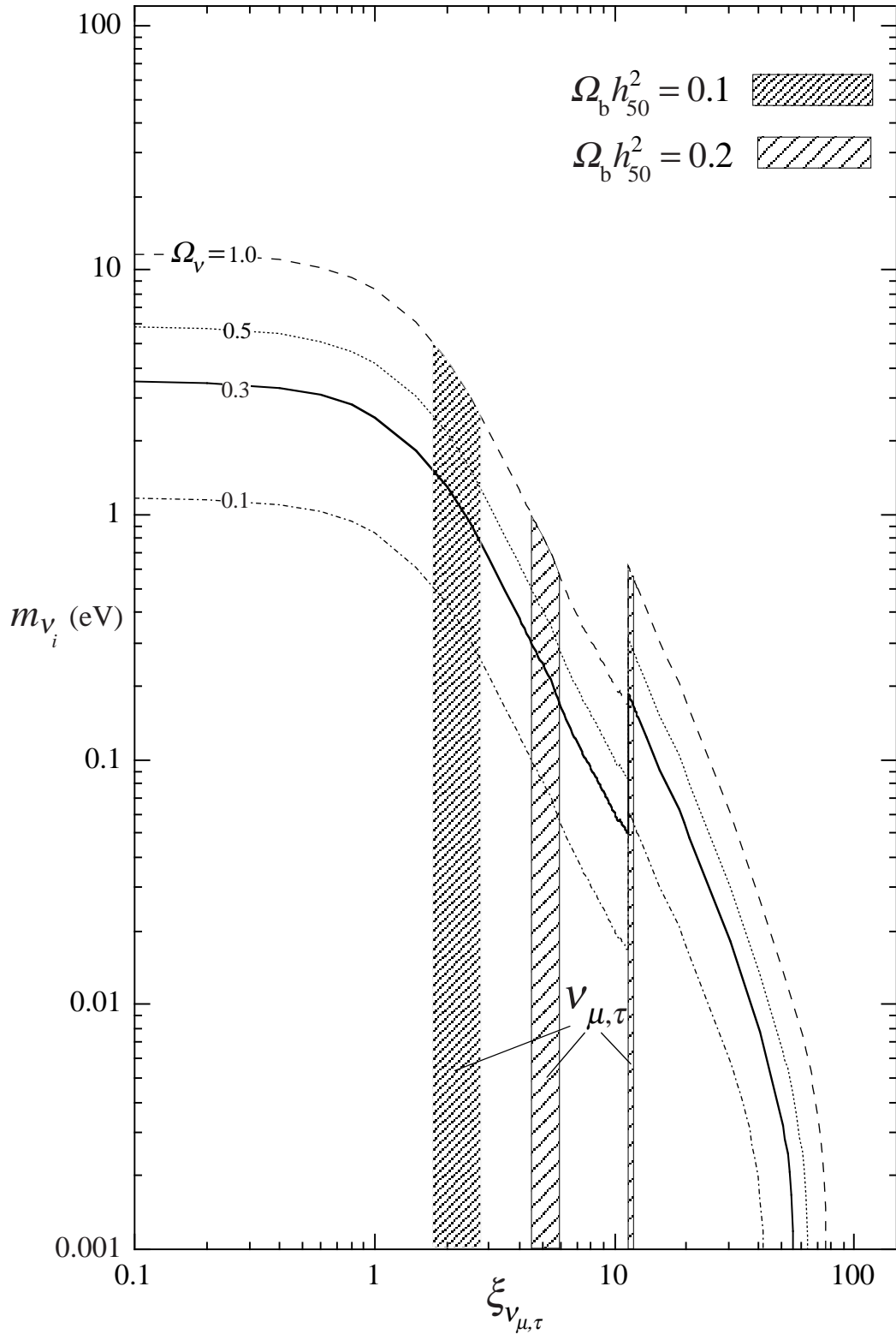


Fig. 12.— Contours of equal present energy density of massive degenerate neutrinos as a function of the degeneracy $\xi_{\nu_{\mu,\tau}}$ and neutrino mass m_ν for $\Omega_\nu = 0.1, 0.3, 0.5,$ and 1.0 as indicated. Each curve corresponds to different value of Ω_ν as indicated. Shaded regions depict the allowed range of degeneracy for the two indicated values of $\Omega_b h_{50}^2 = 0.1,$ and 0.2 as shown in Fig. 8

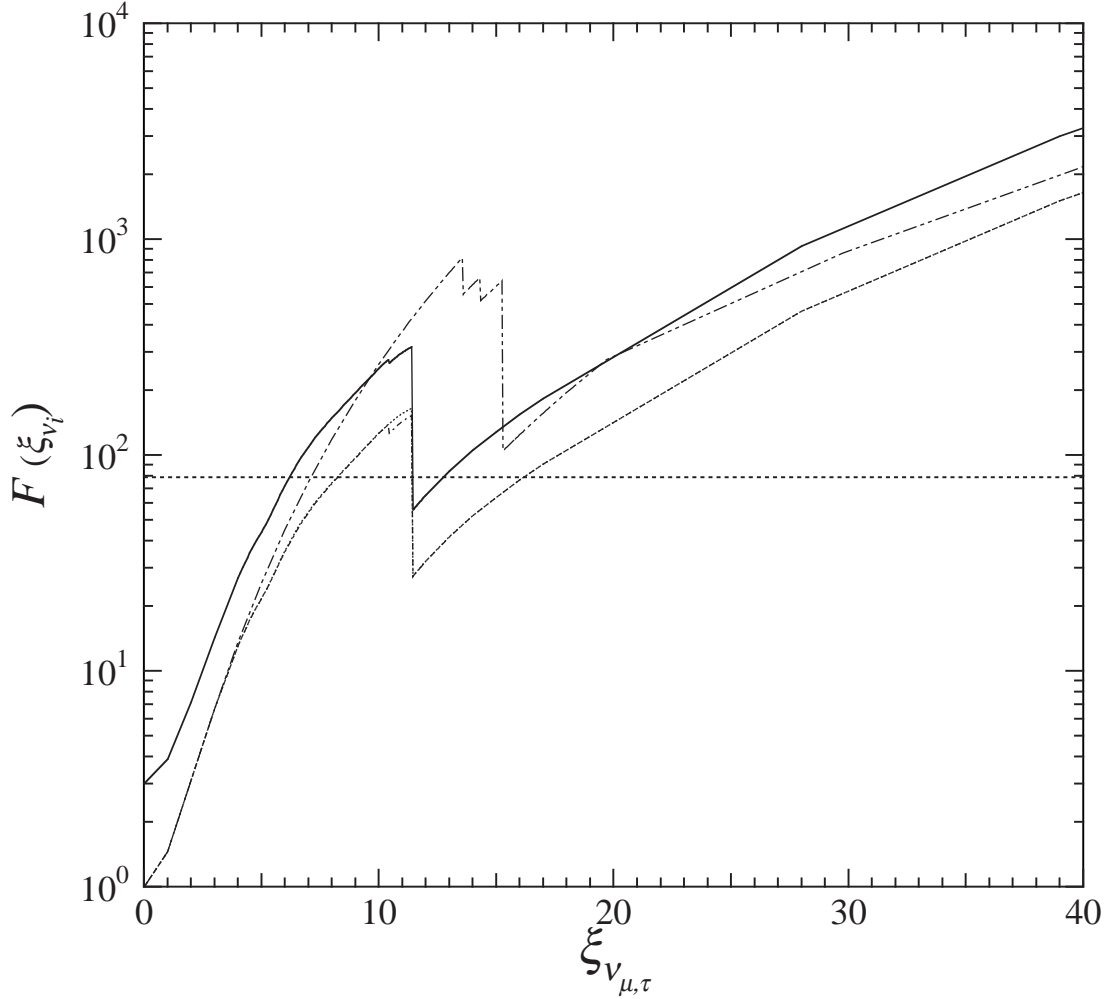


Fig. 13.— Calculated neutrino energy density factors $F(\xi_{\nu_i})$ as a function of degeneracy parameter for the three neutrino species. The dotted and dot-dashed curves display respectively $F(\xi_{\nu_\mu})$ and $F(\xi_{\nu_\tau})$ for the cases in which only one neutrino species is degenerate. Since our interesting parameter regions in Figure 8 satisfy $\xi_{\nu_e} \ll \xi_{\nu_{\mu,\tau}}$, only $\nu_{\mu,\tau}$ contribute significantly to the total $F(\xi_\nu)$ (solid curve). The dashed horizontal line indicates the constraint on neutrino degeneracy from the requirement that sufficient structure develops by the present time. We also show the previous estimate (two-dot dashed curve) of Kang & Steigman (1992).

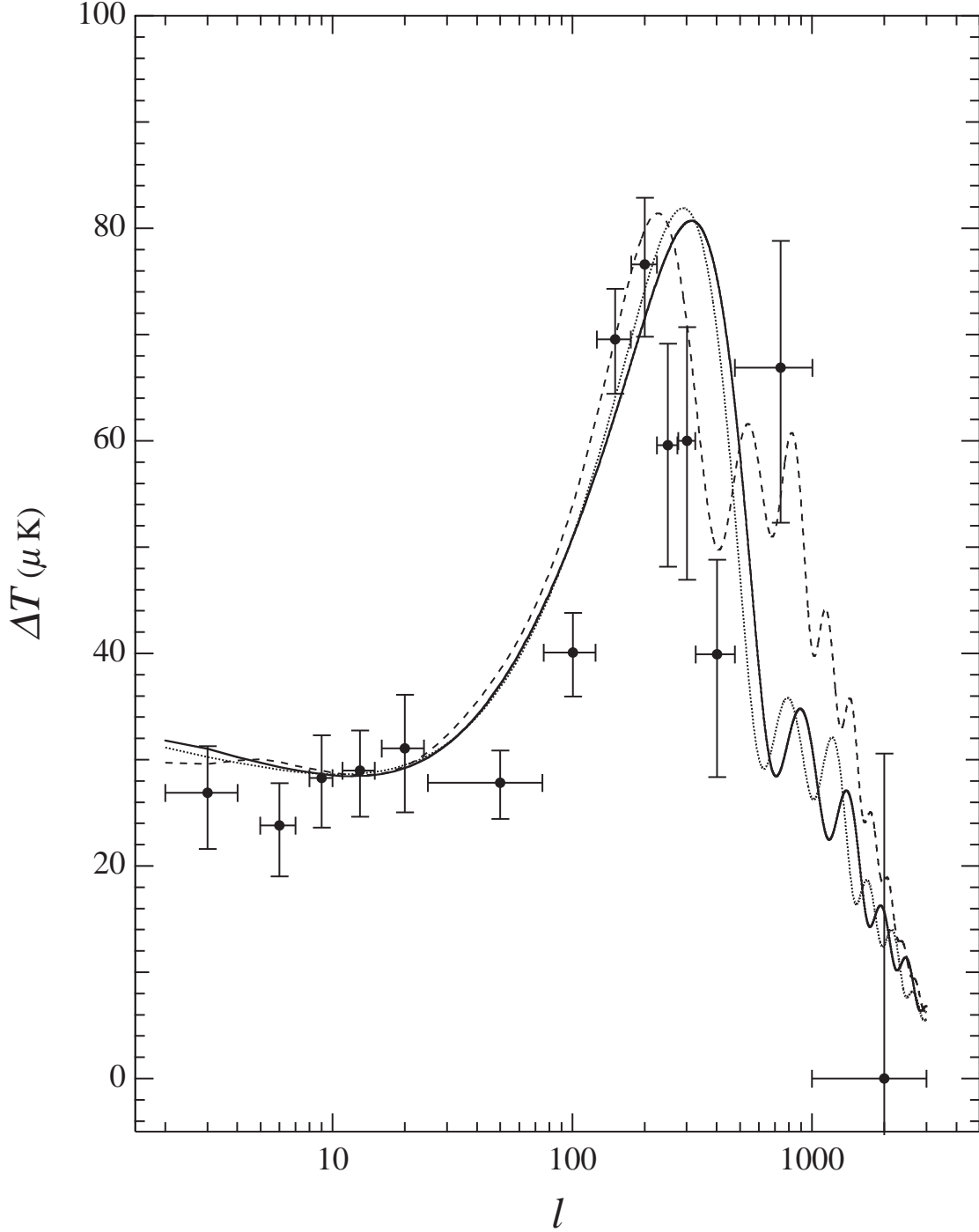


Fig. 14.— CMB power spectrum compared with calculated $\Omega = 1$ models. The points show the binning of 69 experimental measurements based upon the radical compression method of Bond et al. (2000). The dashed line shows the optimum model of Dodelson & Knox (2000). The solid line shows an $\Omega_\Lambda = 0.4$ model with three degenerate neutrinos $\xi_{\nu_{\mu,\tau}} = 11.4$, $\xi_{\nu_e} = 0.73$ and $\Omega_b h_{50}^2 = 0.187$ as described in the text. The dotted line is for an $\Omega_\Lambda = 0$ model with the same degeneracy and baryonic parameters.

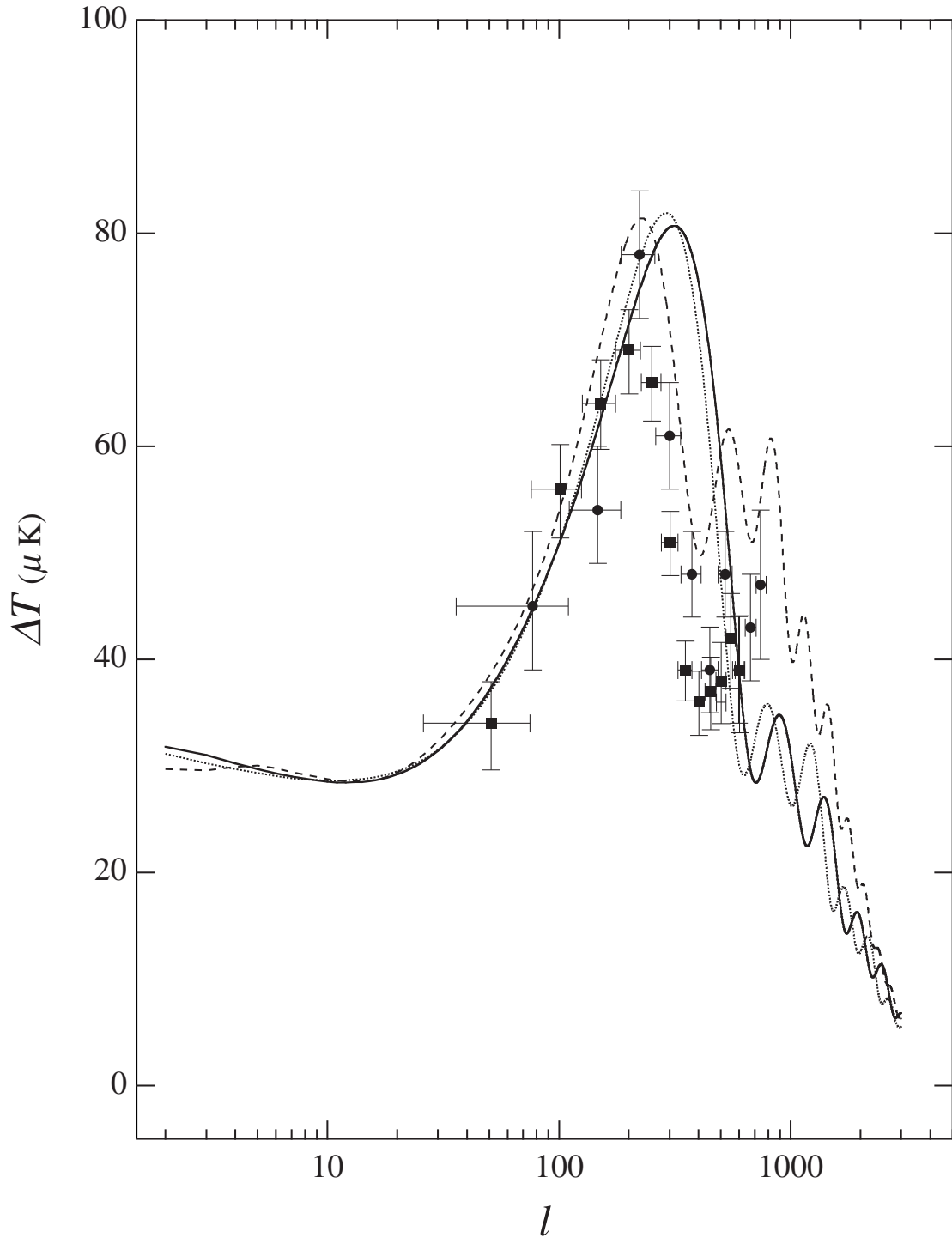


Fig. 15.— CMB power spectrum from the recent MAXIMA-1 (circles) and BOOMERANG (squares) binned data compared with calculated $\Omega = 1$ models of Figure 14. Note that the suppression of the second acoustic peak in the data is consistent with that predicted by the neutrino-degenerate models.